JACS Au
AN OPEN ACCESS JOURNAL OF THE AMERICAN CHEMICAL SOCIETY

pubs.acs.org/jacsau
Perspective

Paired Chemical Upgrading in Photoelectrochemical Cells

Shijie Li, Hongrui Liu, Guangbo Chen,* Li-Zhu Wu, and Tierui Zhang*

Cite This: JACS Au 2025, 5, 2061−2075
Read Online
ACCESS | Metrics & More | Article Recommendations

ABSTRACT: Photoelectrochemical (PEC) technology has emerged as a promising platform for sustainable energy conversion and chemical synthesis, utilizing solar energy to facilitate redox reactions. While PEC systems have been extensively studied for water splitting, CO_2 reduction, nitrogen reduction for value-added compounds synthesis, the sluggish oxygen evolution reaction (OER) on the anode side and the less economic value of O_2 limit system efficiency. To address this, researchers have explored paired chemical upgrading strategies, coupling selective anodic organic oxidation reactions (OORs) with cathodic reduction reactions. This approach enabled the simultaneous production of high-value chemicals and fuels, enhancing the PEC system efficiency and economic viability. In this Perspective, we highlight the latest advancements and milestones in coupling anode OORs and cathode reduction reactions within PEC cells. Particular emphasis is placed on the key design principles, catalyst development, reaction mechanisms, and the performance of paired PEC cells. In addition, challenges and perspectives are provided for the future development of this emerging and sustainable technology.

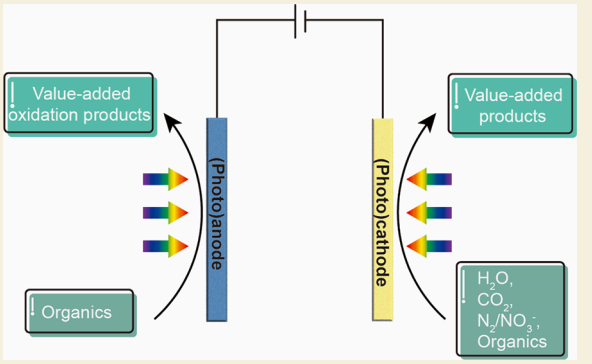

KEYWORDS: *photoelectrocatalysis, paired chemical upgrading, CO_2 reduction, organic oxidation, cathode reduction*

1. INTRODUCTION

Photoelectrochemical (PEC) technology has evolved into a versatile and promising platform for sustainable energy conversion and chemical synthesis by harnessing/utilizing solar energy to drive redox reactions, since the discovery of photoelectric effect.[1] Compared to other green chemistry technologies, PEC technology, on one hand, can be coupled with photovoltaic cells to achieve "full-spectrum utilization," addressing the low quantum yield and the high demand for sacrificial agents associated with photocatalysis.[2−4] On the other hand, PEC technology offers lower costs than traditional electrocatalysis. Additionally, it exhibits superior energy efficiency and stability compared to biocatalysis.[5] In PEC systems, light absorption by a semiconducting photoelectrode generates electron−hole pairs, where holes facilitate oxidation reaction at the anode and electrons drive reduction reaction at the cathode.[6,7] Meanwhile, electrochemistry also plays a crucial role in enabling efficient charge transfer between electrodes and the electrolyte,[8] minimizing energy losses and enhancing reaction performance. Over the past decades, PEC cells have been extensively investigated for applications such as water splitting,[9−15] CO_2 reduction reaction (CO_2RR),[16−18] nitrogen reduction reaction (NRR),[19] and nitrite reduction reaction (NO_3RR).[20−22] By rational design of functional photoelectrode materials, cathode reduction reactions enabled the production of value-added H_2,[23,24] carbon-compounds (e.g., CO, CH_4, CH_3OH, and C_{2+} components),[25] ammonia (NH_3),[26] respectively. Meanwhile, the O_2 molecules were generated on the anode via the oxygen evolution reaction (OER), completing the redox process (Figure 1a). However, the overall PEC efficiency and practicality are often limited by the sluggish O−O coupling process involved in O_2 production and the low economic value of O_2 as a byproduct.[27]

To address the above limitations, researchers have increasingly focused on identifying thermodynamically favorable oxidation reactions to replace the OER process. Recently, PEC organic oxidation reactions (OORs) have attracted increasing attention for valorizing simple organic substances. Remarkably, OORs are both thermodynamically and kinetically more favorable than the OER, as they have lower theoretical equilibrium potentials. By replacing the OER at the anode with OORs, paired PEC systems are created, providing opportunities for the simultaneous production of fuels and value-added chemicals at both the cathode and anode.[28] For instance, alcohols can be selectively oxidized into aldehydes or carboxylic acids, and amines can be converted into imines or nitriles.[29−31] Similarly, biomass derivatives, such as glycer-

Received: January 31, 2025
Revised: March 25, 2025
Accepted: March 27, 2025
Published: April 23, 2025

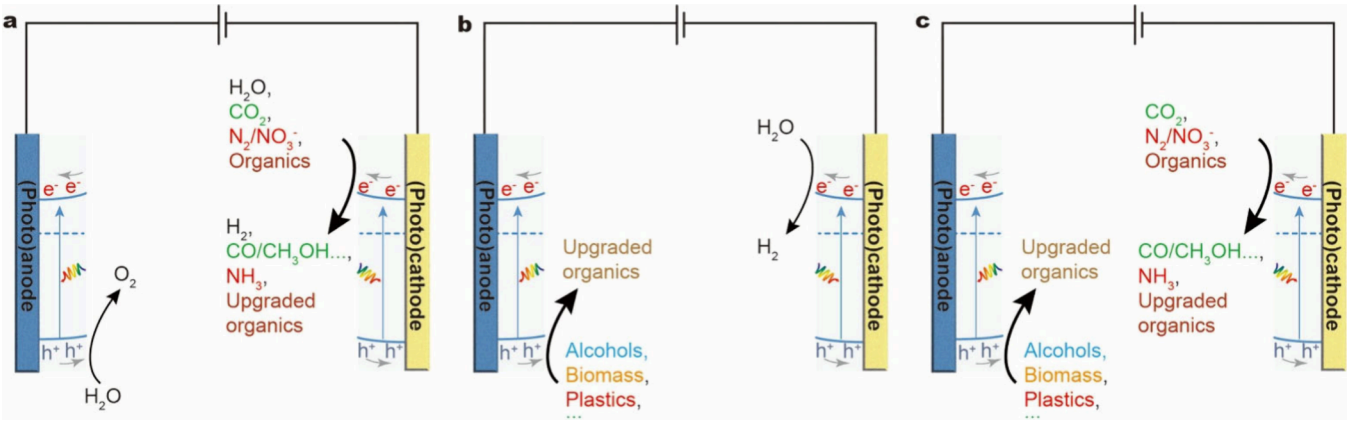

Figure 1. Schematic representation of (a) PEC systems for reduction reactions-OER, (b) PEC systems for HER-OORs and (c) paired PEC systems for -reduction reactions-OORs.

ol[32,33] or glucose,[34] can be upgraded into fine chemicals, adding significant economic value to the process. Other substrates, including C−H bonds,[35−40] sulfides,[41] and alkenes,[42−46] have also been successfully converted into high-value chemicals in PEC systems. These systems typically produced H_2 on the cathode via the hydrogen evolution reaction (HER) from water splitting (Figure 1b). In addition to HER from the water splitting, the PEC dehydrogenation of organic substrates in organic media could also release H_2. The representative examples include PEC C−H functionalization and R^1-H/R^2-H cross-coupling, such as amination,[47] phosphorylation,[39,48] enantioselective cyanation,[49,50] alkylation,[51,52] alkenylation arylation,[53] [2 + 2] cycloaddition,[54] and α-oxyamination.[55] These advancements demonstrate the versatility and efficiency of PEC technology for sustainable H_2 fuel production and chemical upgrading. Such PEC HER-OOR coupling systems have been systematically discussed in a number of excellent review papers, examining both the design of the photoelectrode and the exploration of underlying reaction mechanisms.[56−58] In recent years, the coupling of OORs with processes such as CO_2RR, NRR, and NO_3RR has also garnered increasing attention,[59] empowering the simultaneous conversion of small resource molecules and upgrading of organic substrates (Figure 1c).

In this Perspective, we provide an overview of the latest advancements in coupling anode OOR and cathode reduction reactions within PEC cells. Innovations emphasize the integration of selective oxidation and reduction reactions, enabling the efficient utilization of solar energy for the simultaneous coproduction of high-value chemicals. We place particular emphasis on the design of coupled systems, focusing primarily on CO_2RR, NRR, NO_3RR, and various organic reduction reactions on the cathode, paired OOR on the anode. For each system, we discuss the key design principles, catalyst development, reaction mechanisms, and the performance of paired PEC cells. Furthermore, we address the challenges and provide perspectives for the future development of these emerging coupled systems. Our goal is to provide a state-of-the-art update on innovative coupled chemical upgrading technologies and highlight their significant potential for advancing future sustainable chemical synthesis.

2. COUPLING CATHODIC REDUCTION AND ANODIC OOR FOR CHEMICAL UPGRADING

2.1. CO_2RR-OOR

The increasing concentration of CO_2 in the atmosphere, primarily from fossil fuel combustion and industrial activities, has become a major driver of global climate change.[60] Effective CO_2 conversion into value-added products presents a sustainable solution to reduce greenhouse gas emissions while addressing the growing demand for renewable energy and chemicals. This approach not only mitigates CO_2 accumulation but also transforms it into fuels (e.g., methane, methanol) and valuable chemical feedstocks (e.g., carbon monoxide, ethylene, and formate), contributing to a circular carbon economy.[61,62] PEC CO_2 reduction offers an energy-efficient pathway for CO_2 conversion. Since Halmann's pioneering work in 1978, demonstrating CO_2 reduction using p-type GaP photocathodes,[63] significant progress has been made in PEC CO_2RR over the last decades. These advancements have enabled the successful production of various value-added carbon-based products on the photocathodes, including CO,[64−68] HCOOH,[69−71] CH_3OH,[64,72−74] CH_4,[75] C_2H_4,[76,77] C_2H_5OH,[78,79] and CH_3COOH.[80] Concurrently, the anodic reactions in these systems typically involve water oxidation, leading to the generation of O_2.[31,81,82]

In 2021, Bharath et al. introduced and verified an innovative dual-functional paired PEC system that coupled CO_2RR with OOR.[83] In this system, CH_3OH was produced via PEC CO_2RR on a plasmonic Au/α-Fe_2O_3/reduced graphene oxide (RGO) photocathode. Simultaneously, 2-furoic acid and 5-hydroxyfuroic acid were generated on a Ru/RGO/Pt electrode through the anodic oxidation of furfural. Later on, growing attention has been directed toward the development and exploration of this emerging paired strategy. These CO_2RR-OOR systems have enabled the efficient conversion of CO_2 at the (photo)cathode while simultaneously upgrading simple organic substances at the (photo)anode. For example, in 2022, Reisner and co-workers reported the coupling of CO_2RR to formate with alcohol oxidation to aldehyde in a bias-free PEC device (Figure 2a).[84] The photoanode was fabricated by co-immobilization of a diketopyrrolopyrrole-based chromophore and a nitroxyl-based alcohol oxidation catalyst on a mesoporous TiO_2 ($mTiO_2$) scaffold, thereby providing a noble-metal-free dye-sensitized photoanode. The resultant photoanode was connected to a biohybrid cathode consisting

https://doi.org/10.1021/jacsau.5c00115
JACS Au 2025, 5, 2061−2075

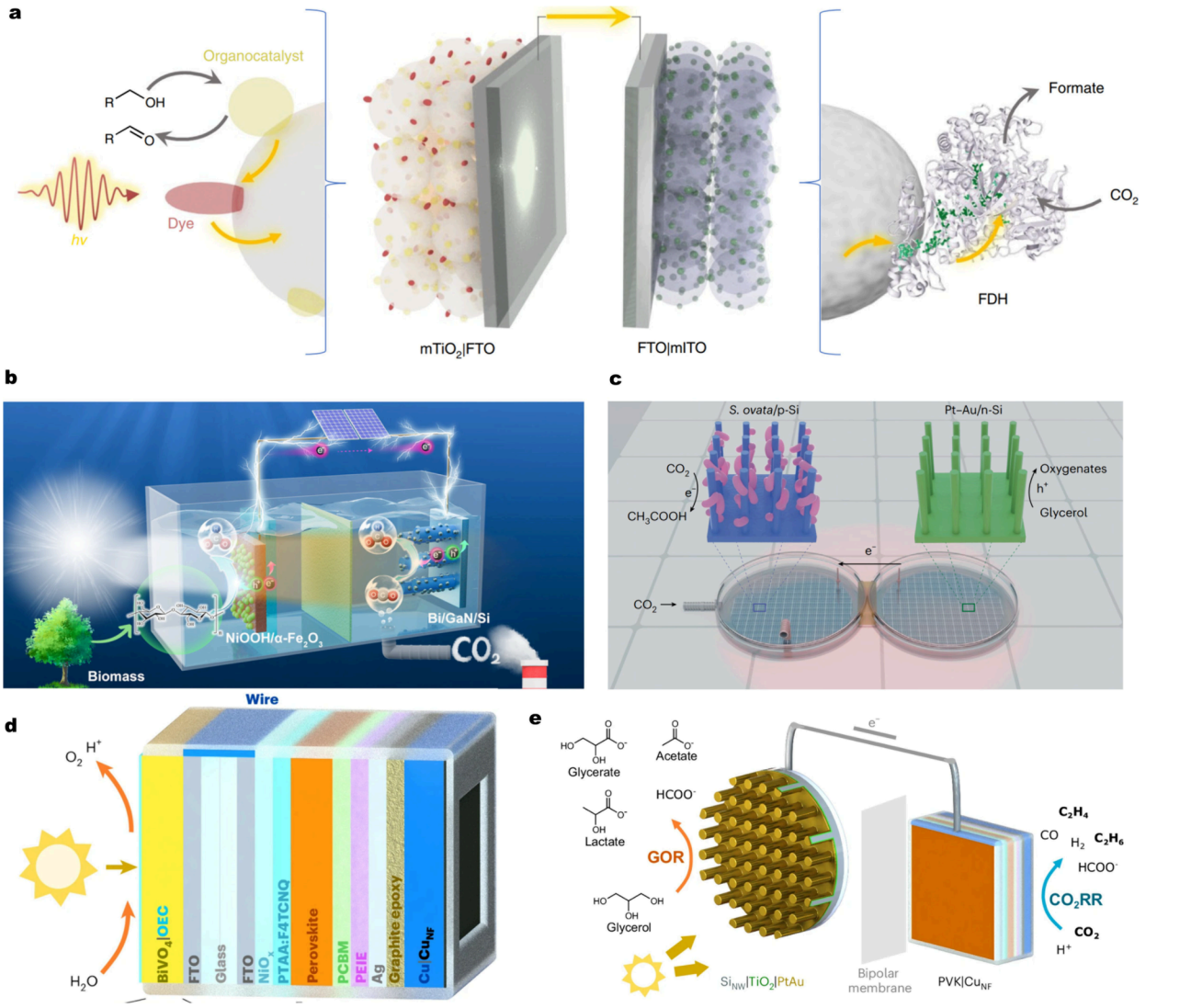

Figure 2. (a) Schematic representation of a fully assembled two-electrode PEC cell for CO_2RR and alcohol oxidation. Orange arrows indicate the electron flow. On light excitation of the dye, an electron was transferred from its excited state to the conduction band (CB) of the $mTiO_2$ semiconductor. The resulting oxidized dye species was quenched by the catalyst, which prompted alcohol oxidation into its corresponding aldehyde. The electron was transferred from the $mTiO_2$ photoanode to the mITO cathode and delivered to FDH, capable of reducing CO_2 to formate. Reproduced with permission from ref 84. Copyright 2022 Springer Nature. (b) Schematic illustration of the tandem PEC cell for formate production from biomass and CO_2. Reproduced from ref 85. Available under a CC-BY license. Copyright 2023 Pan et al. (c) Schematic of a bias-free photochemical diode device consisting of a photocathode and a photoanode separated by a bipolar membrane under red light irradiation. Reproduced with permission from ref 92. Copyright 2024, Springer Nature. (d) Schematic illustration of the perovskite-$BiVO_4$ artificial leaf device toward unassisted C_2 hydrocarbon synthesis at the photocathode. (e) The schematic illustration of the PEC device wiring a nanowire Si photoanode to a PVK|Cu_{NF} photocathode. Reproduced from ref 93. Available under a CC-BY license. Copyright 2025 Andrei et al.

of a W-containing CO_2 reduction enzyme formate dehydrogenase (FDH) on a mesoporous indium tin oxide (mITO) that supported by a mesoporous FTO electrode to form a complete PEC device. This unbiased PEC cell achieved a sustained photocurrent of up to 30 μA cm^{-2} under visible light irradiation, simultaneously reducing CO_2 to formate and oxidizing 4-methylbenzyl alcohol to its corresponding aldehydes. Moreover, they expanded the substrate range to the anode oxidation of 5-(hydroxymethyl) furfural, leading to a current density of 10 μA cm^{-2} with concurrent reduction of CO_2. This study showed that only a single light-absorbing unit could provide sufficient driving force for CO_2RR and OOR, without the need for applied bias and noble metals.

Later on, Pan et al. demonstrated solar formate production by coupling CO_2RR with the oxidation of readily available biomass waste (i.e., glucose), utilizing Bi/GaN/Si wafer photocathode and NiOOH/α-Fe_2O_3 photoanode (Figure 2b).[85] This coupled CO_2RR- biomass oxidation PEC system reduced the cell voltage by 32% compared with traditional CO_2RR-OER PEC cell. Eventually, it achieved Faraday efficiencies (FEs) exceeding 100% for formate generation, with a record yield of 23.3 μmol cm^{-2} h^{-1}. Moreover, the system showed excellent stability, maintaining continuous operation for 10 h without obvious performance decline.

In addition to glucose oxidation, this concept has also been applied to coupling CO_2RR with glycerol oxidation, another important feedstock molecular derived from biomass or byproduct of biodiesel production.[33,86−91] In 2024, Kim et al. reported a photochemical diode device capable of using red light (740 nm) to simultaneously drive photoanodic glycerol

https://doi.org/10.1021/jacsau.5c00115
JACS Au 2025, 5, 2061−2075

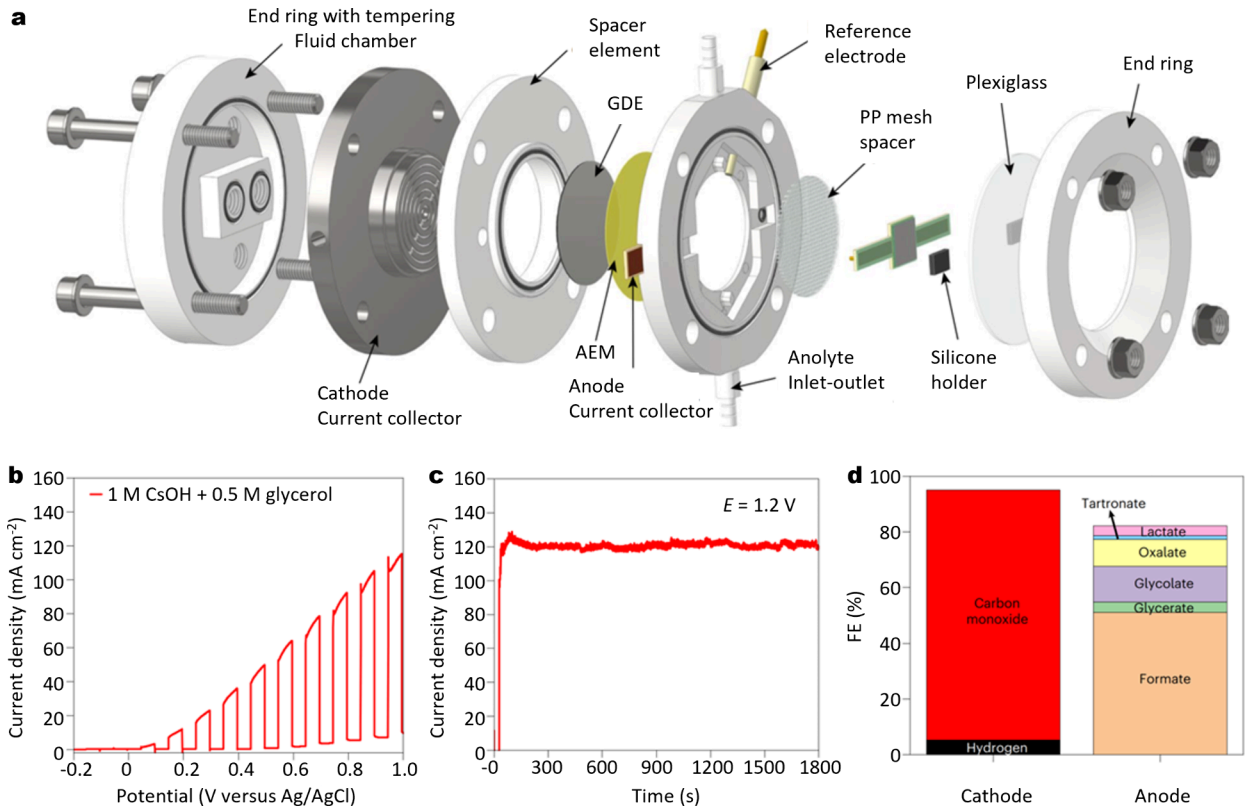

Figure 3. (a) Exploded schematic view of the PEC flow cell for coupling CO_2RR with GOR. (b) Photovoltammogram of a Ni-covered Si photoanode for GOR. (c) Potentiostatic measurement at 1.0 V vs Ag/AgCl anode potential for 30 min. (d) Cathode and anode product distribution at 1.0 V vs Ag/AgCl. The experiments were conducted using a solar simulator (AM 1.5) as the light source operated at 1000 mW cm^{-2}. The anolyte was 0.5 M glycerol containing 1.0 M CsOH. CO_2RR was performed on the cathode side using 25 mL min^{-1} CO_2 flow, while the anolyte was non-recirculated, and the flow rate was 2 mL min^{-1}. The temperature of the cell and the anolyte was 35 °C. Reproduced from ref 94. Available under a CC-BY license. Copyright 2024 Balog et al.

oxidation reaction (GOR) and biophotocathodic CO_2RR to acetate.[92] As shown in Figure 2c, the device comprised the highly efficient CO_2-fixing microorganism (i.e., *Sporomusa ovata*) integrated with a p-type silicon nanowire photocathode (S. ovata/p-Si) and a platinum−gold-loaded n-type silicon nanowire photoanode (Pt−Au/n-Si). Under low-intensity (20 mW cm^{-2}) 740 nm red light-emitting diode (LED) irradiation, the PEC device generated a photovoltage of 0.85 V, which was sufficient to simultaneously drive the biological CO_2RR and GOR. As a result, this silicon p/n-configured photochemical diode delivered a maximum bias-free current density of ∼ 1.2 mA cm^{-2} for PEC CO_2-to-C_2 reduction with a high FE of ∼ 80% for both the cathodic and anodic reactions. The emerging PEC diode devices enabled the efficient conversion of CO_2 into valuable chemicals and the upgrading of glycerol by synergistically utilizing light energy through highly efficient CO_2-fixing microorganisms and abundant silicon materials on the earth. To further enhance the selectivity of CO_2 reduction to C_2 products (C_2H_4, C_2H_6, etc.) in a bias-free coupling system, Yang's team designed an innovative PEC device. This PEC device featured a Cu nanoflower catalyst interfaced with perovskite PV devices using graphite epoxy paste to form buried-junction photocathodes (abbreviated as PVK|CuNF), which served as the photoelectrocathode for CO_2 reduction (Figure 2d). Meanwhile, the photoanode was constructed by wiring the perovskite photocathodes to Si photoanodes for GOR (Figure 2e). This unassisted perovskite-silicon PEC device attained partial C_2 hydrocarbon photocurrent densities of 155 μA cm^{-2}, which was ∼ 200 times higher than that of conventional perovskite-$BiVO_4$ artificial leaves used for water and CO_2 splitting. Moreover, the resulting perovskite photocathodes exhibited a 9.8% Faradaic yield toward C_2 hydrocarbon production at 0 V vs reversible hydrogen electrode (RHE).[93]

The above examples highlighted the successful coupling of CO_2RR with OOR, offering a sustainable pathway to mitigate excessive CO_2 emissions while efficiently producing valuable chemicals from CO_2 and simple organic precursors. However, these studies were typically conducted in an "H-cell", where catalytic efficiencies were limited by slow mass transfer, posing a significant challenge to the scale-up and industrialization of PEC chemical upgrading technology. In response to this challenge, Janáky and co-workers proposed a membrane (i.e., anion-exchange membrane, AEM)-separated continuous-flow PEC cell featuring an n-Si photoanode and the gas diffusion electrode (GDE) cathode, which was employed for pairing CO_2RR and GOR.[94] As shown in Figure 3a, this continuous-flow PEC cell featured an innovative design enabling front-side illumination in PEC experiments, accommodating opaque substrates, and broadening the range of suitable semiconductors. Photovoltammetry tests indicated that the onset potential for glycerol oxidation was approximately 0 V vs Ag/AgCl (Figure 3b). With increasing bias, the photocurrent increased and exceeded 110 mA cm^{-2}, much higher than the values previously reported for PEC GOR (<10 mA cm^{-2}). The constant potential test at 1.0 vs Ag/AgCl showed excellent

https://doi.org/10.1021/jacsau.5c00115
JACS Au 2025, 5, 2061−2075

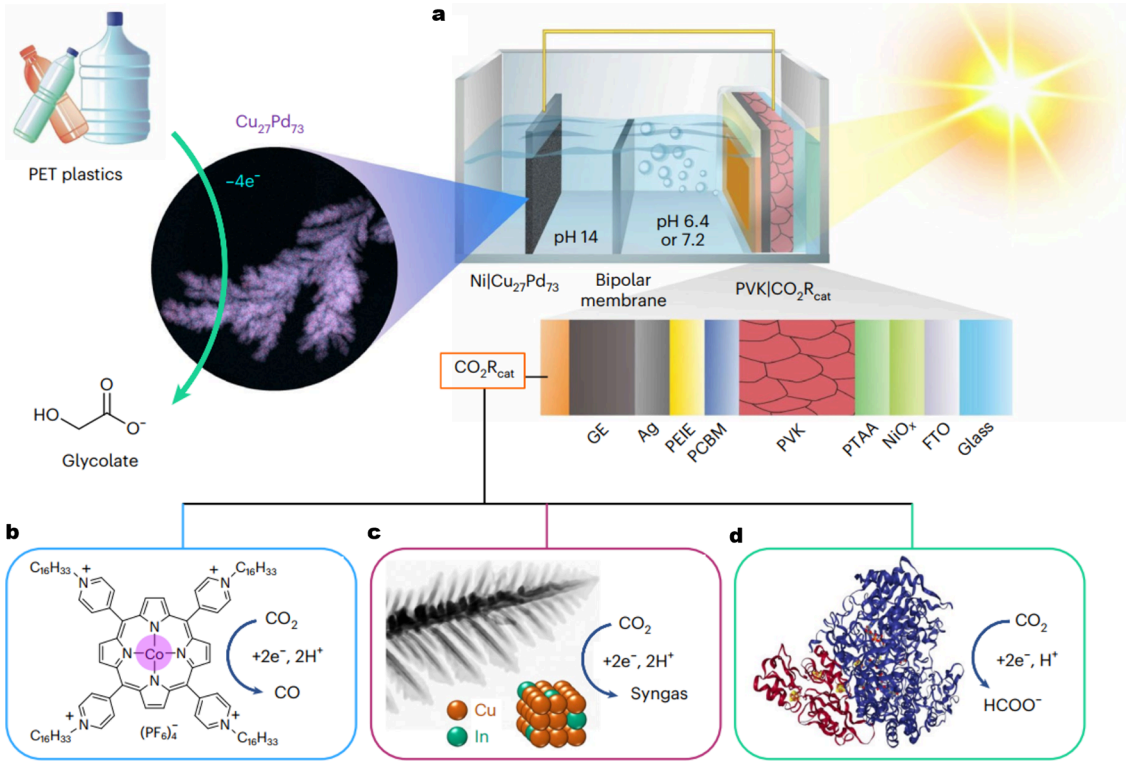

Figure 4. PEC cell demonstration for CO_2-to-fuel production coupled with plastic reforming. (a) Schematic representation of the two-compartment $Cu_{27}Pd_{73}||PVK|CO_2R_{cat}$ PEC system. The system with different CO_2RR catalysts, (b) CoP_L, (c) $Cu_{91}In_9$, and (d) FDH. Reproduced with permission from ref 112. Copyright 2022 Springer Nature.

stability of the PEC device (Figure 3c). The FE of the cathodic CO_2RR was nearly 100%, with 95% for CO and 5% for H_2. Meanwhile, the FE of the anode GOR was calculated to be ~85%, with mixed product formation including formate, glycerate, glycolate, oxalate, tartronate, and lactate, surpassing values reported in the existing literature (Figure 3d). This study established a new research paradigm for the design and mechanistic exploration of PEC continuous-flow cells.

2.2. CO_2RR-Plastic Oxidation

Plastics have become indispensable in various industries and daily life due to their versatility and durability. However, their indiscriminate disposal and inadequate waste management have led to a severe global environmental and ecological crisis.[95] Currently, plastic waste is predominantly managed through incineration and landfilling, which not only generate minimal value-added products but also cause significant environmental pollution. A more sustainable alternative strategy is plastic recycling and upgrading, which can be achieved through two primary methods: mechanical recycling and chemical processing.[96,97] Due to the progressive degradation of structural properties with each recycling cycle, mechanical recycling typically results in downcycling, yielding lower-value products, such as carpets and building materials. Additionally, its applicability is restricted to uncontaminated, single-component thermoplastics, limiting broader implementation. In contrast, chemical recycling often relies on harsh reaction conditions and highly toxic reagents, posing challenges to sustainability and contradicting the principles of green development.[98,99] The catalytic approaches (e.g., photochemical and electrochemical methods) enable efficient upcycling of plastic waste into value-added chemicals, aligning with the principles of environmentally sustainable development. Furthermore, these catalytic strategies possess unique capability for selective activation of specific functional groups, thereby achieving exceptional product selectivity during the transformation process. Therefore, recently, photo- and electrocatalytic technologies, driven by renewable energy under mild conditions, have garnered significant attention, offering a promising solution for sustainable plastic management.[100−103] PEC upgrading technologies retain various advantages of photo- and electrocatalysis and remove restrictions among different technologies. In recent years, PEC polyethylene terephthalate (PET) oxidation reforming has successfully been realized on several common photoelectrodes, including Ni-Pi/α-Fe_2O_3,[104] Ti−Fe_2O_3/Ni-$(OH)_x$,[105] $Cu_{30}Pd_{70}$/perovskite/Pt,[106] Fe_2O_3/$Ni(OH)_x$,[107] Co_3O_4/NF,[108] and nano-TiO_2/nano−Ni-P[109] and TiO_2-modified boron-doped diamond.[110] The PEC polyimide oxidation reforming can be also achieved on a Ti-doped α-Fe_2O_3 photoanode.[111]

In 2022, Reisner's team innovatively paired solar-driven CO_2RR with plastic reforming for the generation of value-added products employing a single-light absorber with no applied bias.[112] As depicted in Figure 4a, lead halide perovskite devices (PVKs) were employed in the coupling system as perovskites could be used as efficient light absorbers and be seamlessly integrated with encapsulation as part of the photocathode in the PEC architecture. In addition, three distinct types of CO_2RR catalysts (CO_2Rcat) were integrated with a perovskite light absorber to form the photocathodes. These catalysts included a lipophilic alkyl-functionalized cobalt porphyrin (CoP_L) molecular catalyst, a copper−indium ($Cu_{91}In_9$) bimetallic alloy, and a tungsten-based FDH derived from *Desulfovibrio vulgaris* Hildenborough (Figure 4b-d). A

https://doi.org/10.1021/jacsau.5c00115
JACS Au 2025, 5, 2061−2075

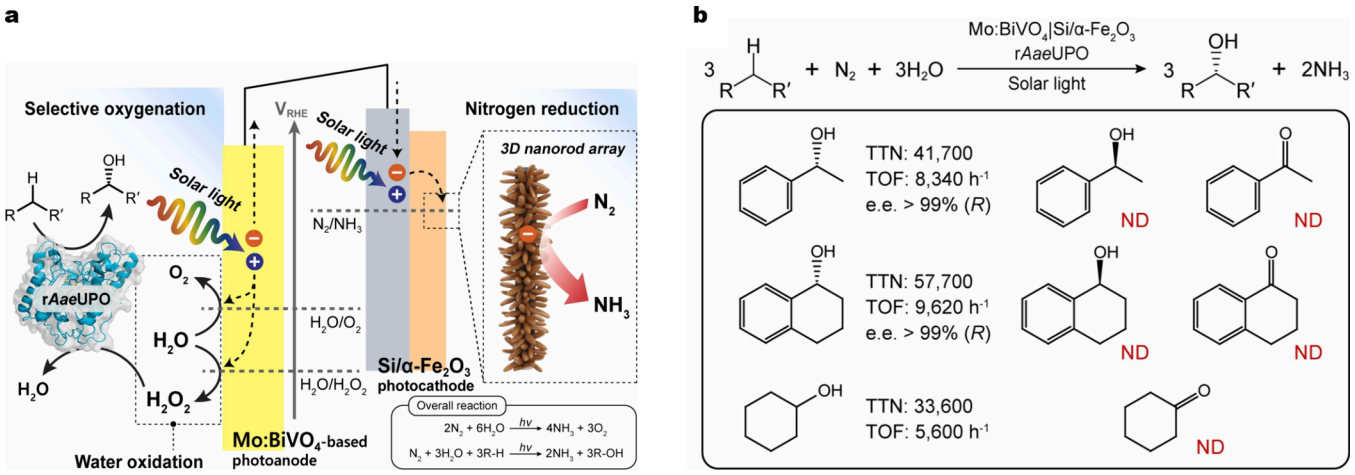

Figure 5. (a) Schematic illustration of unbiased paring of NRR with enantioselective enzymatic synthesis. A Si/α-Fe_2O_3 photocathode reduced N_2 to NH_3 while a water-oxidizing Mo:$BiVO_4$-based photoanode extracted electrons from H_2O as an electron donor. Si/α-Fe_2O_3 was electrically connected to Mo:$BiVO_4$ for producing NH_3 and H_2O_2 at cathodic and anodic sites, respectively. The in situ generated H_2O_2 activated r*Aae*UPO for enantioselective oxyfunctionalization reactions. (b) The PEC performance of r*Aae*UPO-driven oxygenation reactions on the Mo:$BiVO_4$|Si/α-Fe_2O_3 coupling with NRR. Reproduced with permission from ref 120. Copyright 2023 Elsevier.

bimetallic $Cu_{27}Pd_{73}$ alloy was employed as an anode catalyst to form a $Cu_{27}Pd_{73}$||PVK|CO_2R_{cat} PEC device. Remarkably, the $Cu_{27}Pd_{73}$||PVK|CoP_L, $Cu_{27}Pd_{73}$||PVK|$Cu_{91}In_9$, and $Cu_{27}Pd_{73}$||PVK|FDH cells selectively produced CO, syngas, and formate on the photocathode via CO_2RR, respectively. Concurrently, value-added glycolic acid (GA) was generated at the $Cu_{27}Pd_{73}$ anode through the oxidation reforming of real-world PET plastic. Notably, the $Cu_{27}Pd_{73}$||PVK| CoP_L cell produced 263 ± 99 μmol cm^{-2} of CO after 10 h at zero applied voltage, with a high FE of ∼ 90%. The turnover number for CO (TON_{CO}) and turnover frequency (TOF_{CO}) were estimated to be 1.1 × 10^4 and 0.3 s^{-1}, respectively. GA was produced at the anode with a yield of 31 ± 7 μmol and a FE_{GA} of 98 ± 0.3%. This work provided a novel demonstration of solar-driven, selective CO_2RR integrated with the valorization of plastic waste for the generation of valuable chemicals.

2.3. NRR-OOR

The reduction of N_2 into NH_3 is critical for supporting global food production and chemical manufacturing as NH_3 serves as a key feedstock for fertilizers, fuels, and other chemicals.[113] Traditionally, the Haber-Bosch process has been used to synthesize ammonia, but it is highly energy-intensive, consuming approximately 1−2% of global energy and contributing significantly to greenhouse gas emissions.[114,115] Therefore, developing sustainable and energy-efficient alternatives for N_2 reduction is essential. In 2016, Ali et al. first reported solar-driven PEC NRR using a plasmon-assisted Si photocathode with Au nanoparticles (NPs), achieving a high NH_3 production rate of 13.3 mg m^{-2} h^{-1} under 2 sun irradiation.[116] Subsequently, Gong and co-workers promoted PEC NRR to NH_3 by integrating surface oxygen vacancies (O_{vac}) and plasmonic Au NPs into TiO_2/Au/a-TiO_2 photoelectrodes.[117] Wu's group further advanced the field by demonstrating PEC NRR without applied bias using an Ag-loaded black Si photocathode, generating NH_3 with a high yield (2.87 μmol h^{-1} cm^{-2}) and FE (40.6%).[118] Further advancements in photocathode engineering and cell design have improved the performance of PEC NRR systems.[53,119]

In 2023, Park and his colleagues reported an unbiased pairing of NH_3 production from NRR with enantioselective oxyfunctionalization aided by enzyme chemistry using a Mo:$BiVO_4$|Si(1.80 V)/α-Fe_2O_3 PEC device.[120] As illustrated in Figure 5a, both Mo: $BiVO_4$ and Si photoelec trodes absorbed solar energy to generate photoexcited electrons and holes, resulting in the corresponding quasi-Fermi levels of electrons ($E_{f,n}$) and holes ($E_{f,h}$). The Mo:$BiVO_4$ photoanode transferred its photoexcited holes to H_2O, producing H_2O_2. The generated H_2O_2 was then utilized by *Agrocybe aegerita* (r*Aae*UPO), forming the catalytically active oxoferryl heme, which facilitated enantioselective oxygenation reactions. Simultaneously, the photoexcited electrons from Mo:$BiVO_4$ recombined with the photoexcited holes from the Si photovoltaic (PV) layer, while the Si PV's photoexcited electrons were transferred to the conduction band of α-Fe_2O_3. These excited electrons drove the N_2-to-NH_3 conversion at the surface of α-Fe_2O_3, completing the paired process of NH_3 production and enantioselective oxyfunctionalization. As a result, this system selectively hydroxylated ethylbenzene to enantiopure (*R*)-1-phenylethanol [>99% enantiomeric excess (e.e.)], achieving a turnover frequency for r*Aae*UPO ($TOF_{rAaeUPO}$) of 8340 h^{-1} and a total turnover number of r*Aae*UPO ($TTN_{rAaeUPO}$) of 41700 in the anodic site. Simultaneously, N_2 was reduced to NH_3 at a rate of 1.38 μg h^{-1} at the cathodic site. Remarkably, the NRR could also be coupled with other enantioselective hydroxylation reactions in this cell, such as tetralin and cyclohexane, achieving >99% e.e., along with high TOF and TON values (Figure 5b). This work established a novel platform for unbiased chemical synthesis utilizing N_2, H_2O, and sunlight as sustainable inputs. However, it is clear that NH_3 generation remains extremely low, highlighting the need for catalyst discovery and optimization to further enhance the NH_3 production rate.

2.4. NO_3RR-OOR

While NO_3^- is an essential component of the nitrogen cycle, excessive nitrate levels in water bodies, primarily from agricultural runoff and industrial waste, lead to severe environmental issues such as water eutrophication and contamination of drinking water, posing risks to human health. NO_3RR offers a promising pathway to mitigate pollution while converting harmful nitrates into valuable products (e.g.,

https://doi.org/10.1021/jacsau.5c00115
JACS Au 2025, 5, 2061−2075

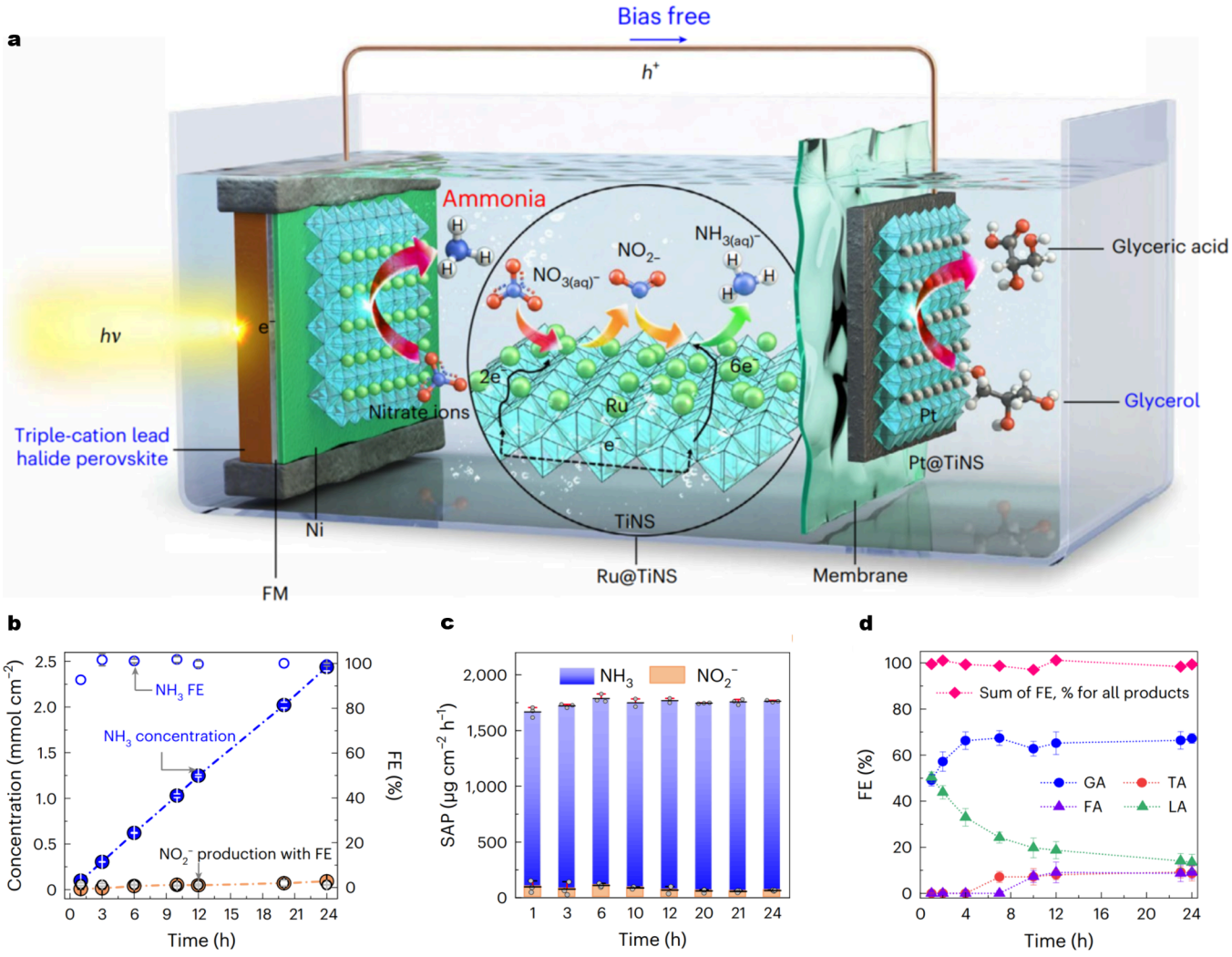

Figure 6. (a) Schematic of the PEC NO_3RR-GOR cell for bias-free NH_3 production and glycerol valorization. (b) Amount of NH_3 generated at the photocathode and corresponding FE throughout a 24 h reaction at 0 V applied bias. (c) Solar-to-ammonia productivity (SAP) statistics toward solar NH_3 and NO_2^- production during a 24 h reaction. (d) FE of GOR products in the bias-free system under continuous operation. Reproduced with permission from ref 133. Copyright 2024 Springer Nature.

NH_3).[121−123] In 2022, Kim et al. demonstrated PEC NO_3RR using a Au-decorated ordered silicon nanowire (O_SiNW/Au) array photocathode, producing NH_3 with a FE of 95.6% at 0.2 V vs RHE.[124] Later on, various photocathodes based on $ZnIn_2S_4/BiVO_4$,[125] $TiO_x/CdS/Cu_2ZnSnS_4$,[126] $CeO_2-C/BiVO_4$,[127] $CoCu/TiO_2/Sb_2Se_3$,[128] $CuSn/TiO_2/Sb_2S_3$,[129] copper-decorated black silicon,[130] and organic p−n junctions,[131] have been developed, achieving efficient NH_3 production rates. In these systems, the anodic side generated O_2 through water oxidation.

In 2022, Song et al. designed a pairing approach by designing a heterostructure photoanode ($CdS/CdIn_2S_4$) and protective photocathode ($TiO_2/AZO/Cu_2O/Au$, AZO=Al doped ZnO) at an artificial PEC cell to drive PEC benzyl alcohol oxidation and NO_3^--NH_3 conversion.[132] The heterostructured photoanode exhibited >98% selectivity for benzaldehyde and >99% FE for benzyl alcohol oxidation at 0.67 V vs RHE. Moreover, the photocurrent density of the photoanode and photocathode-integrated PEC device demonstrated about 2.7 mA cm^{-2} at the working voltage of 2.5 V vs RHE and maintained 95% of the original photocurrent density after continuous irradiation. This work innovatively integrated organic oxidation and NO_3RR in a PEC device, providing insights into the design and construction of subsequent PEC cells. In 2024, Jang and co-workers coupled PEC NO_3RR with GOR to obtain higher economic value.[133] As illustrated in Figure 6a, the PEC NO_3RR-GOR cell consisted of two compartments. On the photocathode side, a light-absorbing perovskite material, $Cs_{0.05}(FA_{0.83}MA_{0.17})_{0.95}Pb(Br_{0.17}I_{0.83})_3$, was paired with Ru@TiNS as the electrocatalyst, enabling selective NO_3RR in a nitrate-containing basic solution. On the anode side, glycerol was oxidized in a basic solution using a Pt@TiNS GOR catalyst. Under AM 1.5 G simulated one-sun illumination, this coupling PEC cell demonstrated a high photocurrent of 21.2 + 0.7 mA cm^{-2}, achieving a solar-to-ammonia productivity of 1744.9 ± 20.6 μg_{NH3} cm^{-2} h^{-1} with a FE of 99.5 ± 0.8% without applying any additional bias (Figure 6b, c). Simultaneously, glycerol was oxidized at the anode for the formation of value-added GA and lactic acid (LA) with FE of 98.1 ± 2.4% (Figure 6d).

Moreover, the PEC cell showed superior stability for 24 h without noticeable degradation. This work presented a novel system for the co-upgrading of contaminants and representa-

https://doi.org/10.1021/jacsau.5c00115
JACS Au 2025, 5, 2061−2075

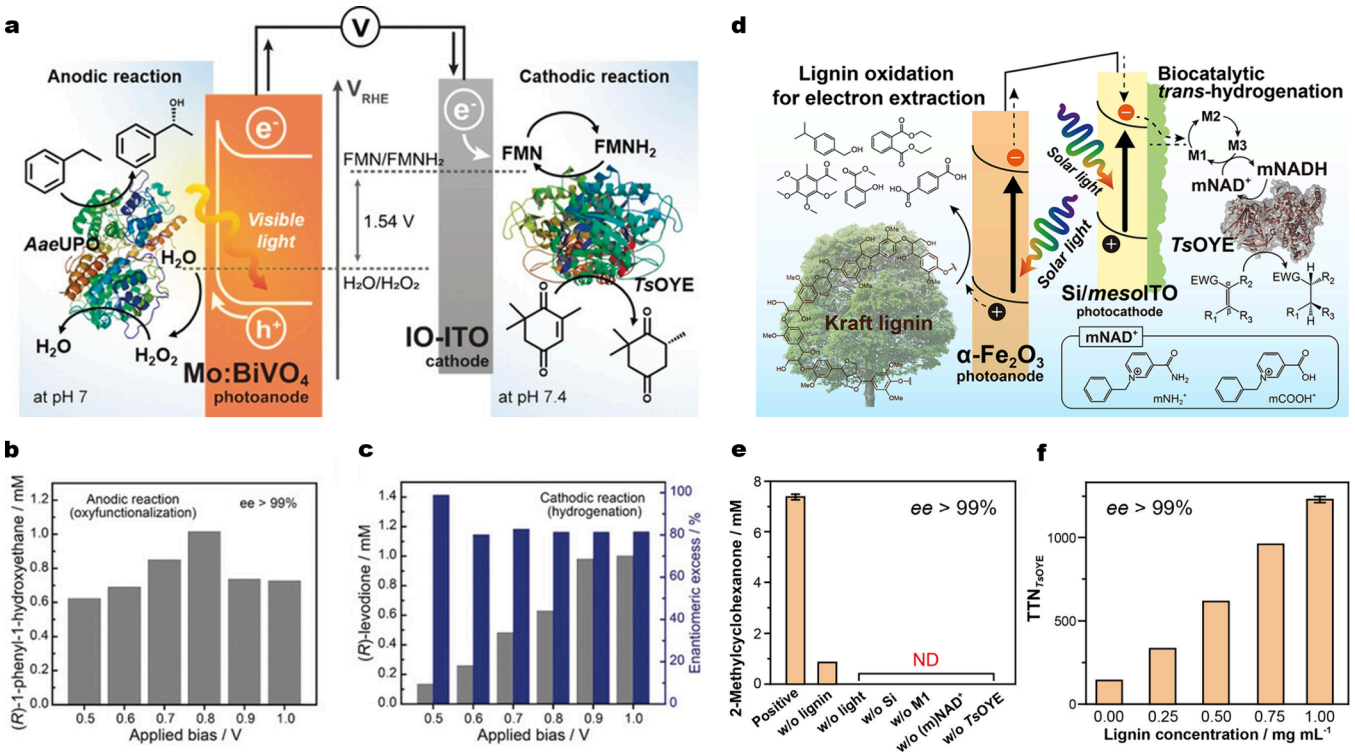

Figure 7. (a) Schematic illustration of the solar-assisted PEC cell for dual biotransformations. (b) (*R*)-1-Phenyl-1-hydroxyethane formation at the 1.0% Mo:BiVO$_4$ photoanode as a function of applied bias for 2 h. (c) (*R*)-Levodione formation and optical purity at the IO-ITO cathode as a function of applied bias for 2 h. Reproduced with permission from ref 136. Copyright 2020 Wiley. (d) Illustration of a PEC platform for bias-free photoelectrocatalytic coupling of lignin oxidation and asymmetric C═C hydrogenation. (e) Control experiments of bias-free biocatalytic PEC hydrogenation of C═C bonds. (f) Effect of lignin concentration on TTN$_{TsOYE}$. Reproduced from ref 137. Copyright 2022 American Chemical Society.

tive biomass-derived waste, enabling the production of valuable compounds.

2.5. Organic Reduction Reaction-OOR

Apart from OOR for organic upgrading, reduction reactions are also commonly employed strategies for upconverting organic substrates, such as hydrogenation reactions and reductive coupling reactions. Similar to the previously discussed paired systems, this approach can be applied to integrate organic reduction reactions with OORs, facilitating the simultaneous upgrading of organic compounds at both the (photo)anode and (photo)cathode. In 2021, Dixit et al. reported the paired oxidation and reduction of biomass-derived furfural to furoic acid and furfuryl alcohol using a Cu−Ni/NF cathode/TiO_2 nanotube photoanode in a PEC cell.[134] They revealed that 0.75 ± 0.02 μmol h^{-1} cm^{-2} of furfuryl alcohol could be generated using TiO_2 photoanode instead of Pt electrode at 1 V applied bias. Furthermore, they designed the flow PEC cell to enhance the paired oxidation and reduction of furfural, optimizing the production rates of furfuryl acid and furfuryl alcohol. This study offered a high-value-added and sustainable pathway for synthesizing platform chemicals. Integrating PEC technology with enzyme chemistry can further enhance catalytic efficiencies, leveraging the high specificity and activity of enzymes. Park and co-workers proposed coupling lignin oxidation and biocatalysis and successfully achieved unbiased lignin decomposition and the biocatalytic reaction of α-ketoglutarate to L-glutamate using a PEC device integrated with a perovskite photovoltaic solar cell. Lignin oxidation was generated at the $BiVO_4$ photoanode, which drove the electroenzymatic reaction at the cathode.[135]

In the same year, they reported a dual biocatalysis PEC platform featuring a molybdenum-doped $BiVO_4$ (Mo:$BiVO_4$) photoanode and an inverse opal ITO (IO-ITO) cathode to drive the coupling of peroxygenase and ene-reductase-mediated catalysis (Figure 7a).[136] Thereinto, photoexcited electrons generated from the Mo:$BiVO_4$ were transferred to the IO-ITO cathode, where they regenerated reduced flavin mononucleotides to drive the ene-reductase-catalyzed trans-hydrogenation of ketoisophorone to (*R*)-levodione. Simultaneously, bias-free photoactivated Mo:$BiVO_4$ produced H_2O_2 in situ via a two-electron water oxidation process, supplying peroxygenases (i.e., *Aea*UPO) to catalyze selective hydroxylation of ethylbenzene into enantiopure (*R*)-1-phenyl-1-hydroxyethane (e.e. > 99%). As shown in Figure 7b, the generation rate of enantiopure (*R*)-1-phenyl-1-hydroxyethane increased with the applied bias (i.e., from 0.5−0.8 V) at the Mo:$BiVO_4$ photoanode. However, the yield began to decline when the bias exceeded 0.8 V, likely due to the competition of biocatalysis and water oxidation at higher biases. On the contrary, the production of (*R*)-levodione by ene-reductase of the Old Yellow Enzyme family from *Thermus scotoductus* (*Ts*OYE) increased with applied bias (Figure 7c). At a bias of 1.0 V, the maximum conversion rate of 0.5 mM h^{-1} with 82% e.e. was achieved. When the applied bias exceeded 0.9 V, only a slight increase in yield was observed, suggesting inefficient energy transfer at the high voltage. This PEC-biocatalysis system showed excellent conversion efficiency with an optimal performance observed at least a bias of 0.8 V. To address dependence on applied bias, a biocatalysis-PEC system with a dual-bandgap configuration has been proposed. In 2022, the

https://doi.org/10.1021/jacsau.5c00115
JACS Au 2025, 5, 2061−2075

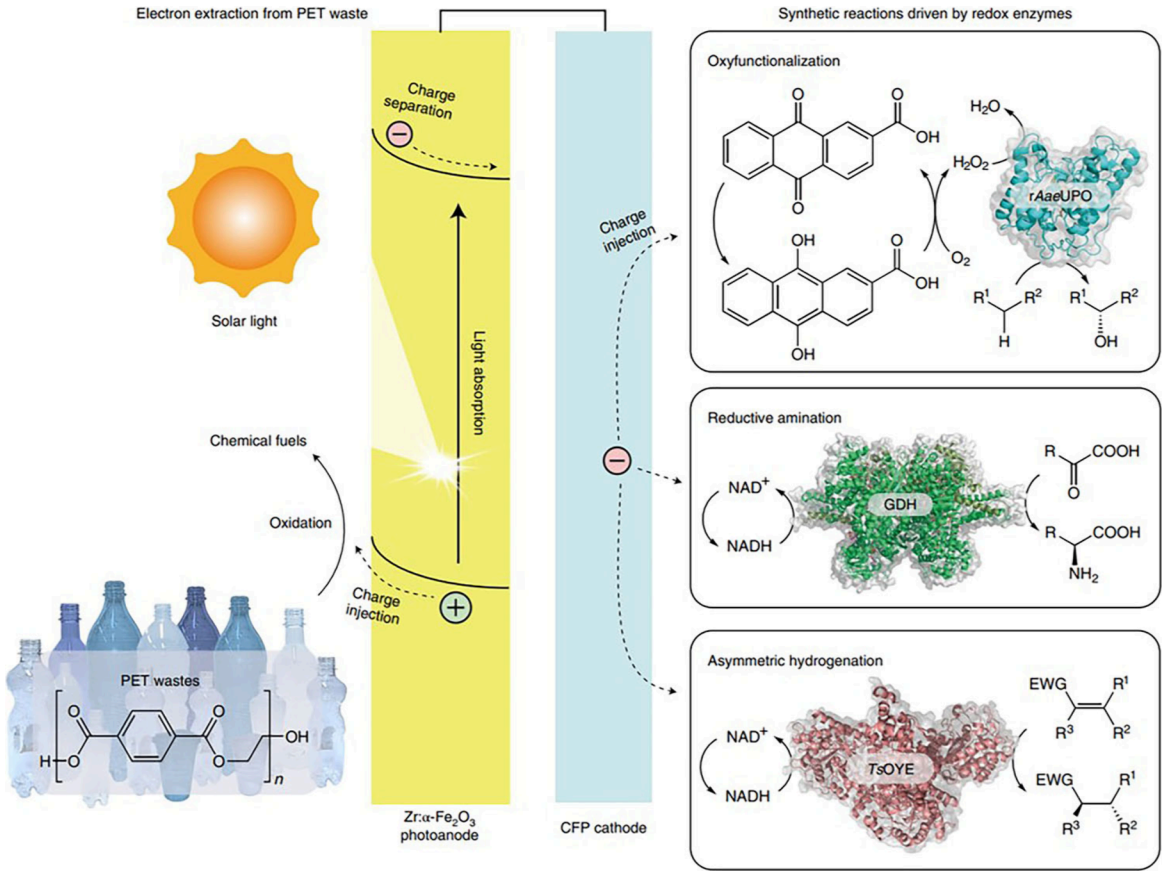

Figure 8. Schematic diagram of solar-powered photoelectrochemical biosynthetic reactions using nonrecyclable real-world PET microplastics. Reproduced with permission from ref 138. Copyright 2022 Springer Nature.

same team reported a bias-free α-Fe_2O_3/Si/mesoporous ITO (α-Fe_2O_3/Si/mesoITO) PEC cell capable of driving lignin oxidation and biocatalysis-mediated enantioselective reduction of α,β-unsaturated hydrocarbons, as illustrated in Figure 7d.[137] In this PEC-biocatalysis system, the asymmetric hydrogenation of the C=C bond required a combination of solar, Si photovoltaic(Si PV), and a photosynthetic unit ([eCp*Rh-(bpy)H_2O]$^{2+}$, **M1**, (m)NAD+, *Ts*OYE) (Figure 7e). The photoanode and photocathode absorbed solar energy, generating charge carriers. Photogenerated holes by α-Fe_2O_3 were utilized for lignin oxidation, while the photogenerated electrons from the Si photocathode were used to reduce **M1**. This reduction facilitated the regeneration of mNADHs, driving *Ts*OYE-catalyzed trans-hydrogenation of conjugated C=C bonds. The lignin oxidation reaction at the photoanode was faster than OER, providing a more electron source to accelerate the hydrogenation reaction. Consequently, TTN_{TsOYE} increased continuously with the rising concentration of anodic lignin (Figure 7f).

This study indicated that lignin-fueled regeneration of superior cofactor analogues offered a renewable and sustainable strategy for efficient biocatalytic photosynthesis, using lignin waste and solar light.

2.6. Organic Reduction Reaction-Plastic Oxidation

The reduction of organic compounds at the cathode can also be coupled with the anodic oxidation of plastic recycling within a PEC system. In 2022, Park and co-workers described a solar-driven PEC-biocatalysis platform that utilized nonrecyclable, real-world PET microplastics as an electron feedstock. This system enabled the synthesis of value-added compounds by combining photoelectrocatalysis with redox biotransformations, including oxyfunctionalization of C−H bonds, amination of C=O bonds, and asymmetric hydrogenation of C=C bonds.[138] As shown in Figure 8, the PEC-biocatalysis system consisted of three key components. First, a zirconium-doped hematite (Zr:α-Fe_2O_3) photoanode was used to extract electrons from hydrolyzed PET solutions derived from postconsumer commercial PET waste. Second, a carbon fiber paper (CFP) cathode or an anthraquinone-2-carboxylic acid-anchored CFP (AQC/CFP) cathode generated either 1,4-dihydronicotinamide adenine dinucleotide (NADH) or H_2O_2, respectively. Third, a redox enzyme, such as NADH-dependent L-glutamate dehydrogenase (GDH), NADH-dependent ene-reductase from the old yellow enzyme (OYE) family, or H_2O_2-dependent unspecific peroxygenase (UPO)-was employed to drive synthetic reduction reactions. The Zr:α-Fe_2O_3|CFP-based systems demonstrated broad applicability to various enzymatic substrates and achieved high total turnover numbers (TTNs) for the enzymes. Under the optimized applied bias for each enzymatic reaction, the photobiocatalytic system achieved a $TTN_{rAaeUPO}$ of 113000 over 3 h, a TTN_{GDH} of 144000 over 56 h, and a TTN_{TsOYE} of 1300 over 7 h. These values significantly exceeded those of state-of-the-art PEC-biocatalysis systems that used water as the electron feedstock. Simultaneously, Zr:α-Fe_2O_3 generated formate and acetate during the PEC reactions via PEC oxidations, highlighting the concurrent production of value-added compounds at both the anodic and cathodic sites.

https://doi.org/10.1021/jacsau.5c00115
JACS Au 2025, 5, 2061−2075

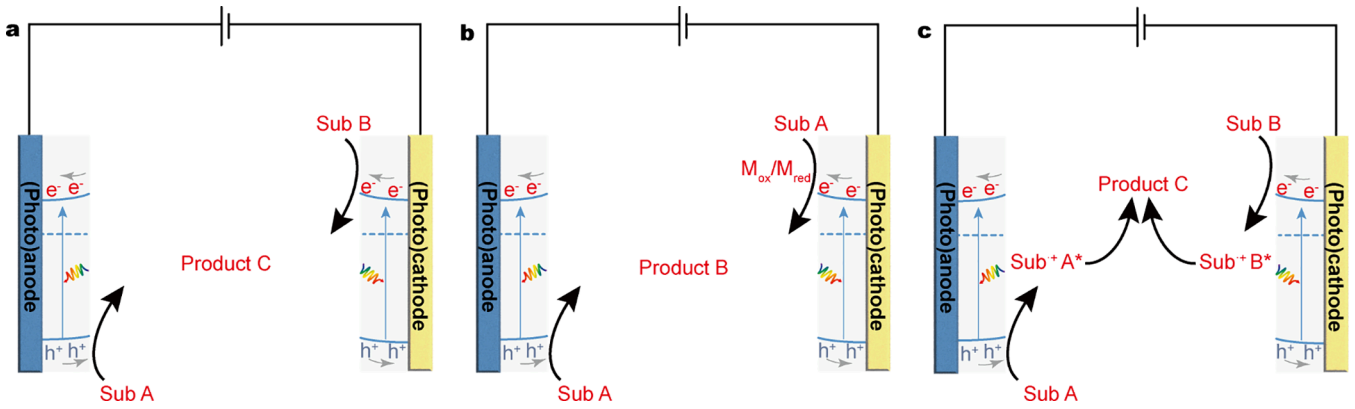

Figure 9. Schematic illustrating the proposed reaction pathways in paired PEC cells for generating a single product. (a) Paired PEC system from different reaction substrates, A → C on the (photo)anode, B → C on the (photo)cathode. (b) Symmetric linear paired PEC system from an identical reaction substrate, A → B on the (photo)anode, A → B on the (photo)cathode mediated by a redox mediator M. (c) Cascade paired PEC system, A → A* on the (photo)anode, B → B* on the (photo)cathode, and then, A* + B* → C.

3. CONCLUSION AND PERSPECTIVES

This Perspective highlights recent advances in cathode reduction reaction coupled with anode OOR in PEC cells. The representative cathodic reductions include CO_2RR, NRR, NO_3RR, and organic reduction reactions. These emerging paired PEC systems open an innovative and sustainable approach to producing high-value-added chemicals. Although the coupling strategy has demonstrated remarkable advantages and achieved significant progress, it is still in its infancy. Challenges such as limited conversion efficiency and narrow substrate range persist. To address these challenges, the rational design of high-performance photoelectrodes, comprehensive mechanism exploration, and intelligent construction of PEC cells will be essential for enabling future industrial applications. Below, we outline our perspectives on the future directions for advancing sustainable paired systems in PEC chemical upgrading.

(1) Stable and efficient semiconductor photoelectrodes are always the prerequisite for the PEC upgrading of chemicals. Currently, commonly used photoelectrode semiconductors (e.g., TiO_2, α-Fe_2O_3, $BiVO_4$, WO_3, and Cu_2O) present limitations, such as poor stability, wide band gaps, and poor light adsorption. To overcome these limitations, effective strategies must be implemented to enhance the light absorption and charge separation efficiencies. These strategies include energy-band engineering, the incorporation of cocatalysts, and the development of hybrid materials. Furthermore, the development of emerging semiconductor photoelectrodes with visible and near-infrared light absorption capabilities along with excellent charge separation and transfer efficiencies will enable more effective utilization of solar energy for chemical upgrading.

(2) The PEC-paired upgrading of chemical compounds is typically a complex process involving multistep chargers and energy transfers as well as intricate interactions during chemical bond breaking and formation. Although great progress has been made in the activation of bonds, such as C−H and O−H, the mechanisms underlying the transformation and energy conversion of many chemical compounds with diverse chemical bonds remain unclear. In addition, compared to single electrode upgrading systems, paired systems require careful consideration of the bias distribution's impact on the reaction process, as it is partially influenced by the properties of the electrodes. Furthermore, a deeper understanding of the structural features of (photo)electrodes, such as crystal structure, morphology, band structure, and surface properties, in relation to their PEC performance, is essential for identifying active sites and elucidating reaction mechanisms. This knowledge is critical for optimizing and designing (photo)electrodes and understanding the reaction mechanism with promoted performance. Achieving this goal required the utilization of advanced characterization techniques to gain detailed insights into the morphology, crystal structure, chemical composition, and electronic properties of photoelectrode materials. In addition, cutting-edge operando techniques, such as in situ X-ray absorption fine structure (XAFS), in situ Raman spectroscopy, and in situ Fourier transform infrared spectroscopy (FTIR) can be used to identify the true active sites and monitor the key intermediates at the atomic level. Furthermore, computational modeling and simulation methods play a vital role in studying structure-performance relationships.

(3) The paired upgrading process in PEC cells should prioritize not only efficiency but also product selectivity. This is particularly important when working with substrates like glycerol, which can yield numerous oxidation products. Ensuring selectivity not only facilitates access to higher-value chemicals but also simplifies the isolation of downstream products. Recent studies have demonstrated that auxiliary physical fields, such as thermal and magnetic coupling, could improve the selectivity and efficiency of PEC reactions. The integration of auxiliary physical fields into the paired PEC systems can significantly enhance the reaction efficiency and improve selectivity.

(4) The economic feasibility of PEC devices cannot be overlooked as they move toward industrialization. Although the pairing of two efficient half-reactions enables high energy utilization efficiency, the economic value of industrial processes is not solely determined by energy efficiency. The separation and collection of products, as well as the atomic utilization of substrates, also play a crucial role in enhancing economic benefits.

https://doi.org/10.1021/jacsau.5c00115
JACS Au 2025, 5, 2061−2075

The convergent paired PEC cells, enabling cogeneration of identical products from distinct substrates in cathodic and anodic cells, offer a promising solution to the technical challenges associated with product separation and collection (Figure 9a). For example, formic acid could be produced from glucose and CO_2.[82] Moreover, the construction of symmetric linear paired PEC cells is emerging to maximize resource and energy utilization (Figure 9b). The linear paired strategy will achieve high atom utilization by producing the same product from a common substrate through different PEC reactions at the electrodes, avoiding the separation of different upgraded chemicals as discussed above. This can be realized by an H_2O_2-mediated catalytic process using O_2 as the oxidant, as employed previously in electrocatalysis.[139,140] Additionally, cascade reactions in paired PEC cells can facilitate new bond formation, enabling the synthesis of valuable chemicals (Figure 9c). For example, through careful system design and optimization, a reduction intermediate can be coupled with an oxidation intermediate within a PEC cell to generate a single target compound. This strategy offers significant potential for C−C bond formation by pairing CO_2 reduction at the cathode with organic oxidation reactions at the anode, utilizing CO_2 as one of the carbon sources. However, a key challenge remains in controlling the lifetime and stability of the reactive intermediates formed at the (photo)anode and (photo)-cathode, including their efficient binding and subsequent coupling.

(5) In terms of scale-up applications, it is necessary to develop a suitable cell configuration that not only delivers high performance but also ensures robustness and safety. The rational design of reactors must address several challenges, including efficient light utilization, enhanced mass transfer, and effective product separation. As mentioned before, continuous-flow cells are promising options, as they can provide a sufficient supply of substrates and facilitate mass transfer. Additionally, systems can be designed for efficient and sustainable organic synthesis through the series configuration of photoanodes and photocathodes or by integrating PEC cells with photovoltaic modules. Furthermore, the economic feasibility of technology, including limitations, downstream separation, and purification processes, needs thorough analysis. Finally, the transition from lab-scale prototypes to industrial-scale production facilities requires careful planning and continuous improvement to ensure scalability, efficiency, and economic viability.

In conclusion, paired chemical upgrading in PEC cells offers a sustainable and cost-effective pathway for green chemical production. With ongoing exploration and innovation, this emerging technology is steadily toward practical application in chemical manufacturing.

AUTHOR INFORMATION

Corresponding Authors

Guangbo Chen − *Key Laboratory of Photochemical Conversion and Optoelectronic Materials, Technical Institute of Physics and Chemistry, Chinese Academy of Sciences, Beijing 100190, P. R. China;* orcid.org/0000-0003-1927-3642; Email: gchen@mail.ipc.ac.cn

Tierui Zhang − *Key Laboratory of Photochemical Conversion and Optoelectronic Materials, Technical Institute of Physics and Chemistry, Chinese Academy of Sciences, Beijing 100190, P. R. China; Center of Materials Science and Optoelectronics Engineering, University of Chinese Academy of Sciences, Beijing 100049, P. R. China;* orcid.org/0000-0002-7948-9413; Email: tierui@mail.ipc.ac.cn

Authors

Shijie Li − *Key Laboratory of Photochemical Conversion and Optoelectronic Materials, Technical Institute of Physics and Chemistry, Chinese Academy of Sciences, Beijing 100190, P. R. China; Center of Materials Science and Optoelectronics Engineering, University of Chinese Academy of Sciences, Beijing 100049, P. R. China*

Hongrui Liu − *Key Laboratory of Photochemical Conversion and Optoelectronic Materials, Technical Institute of Physics and Chemistry, Chinese Academy of Sciences, Beijing 100190, P. R. China; Center of Materials Science and Optoelectronics Engineering, University of Chinese Academy of Sciences, Beijing 100049, P. R. China*

Li-Zhu Wu − *Key Laboratory of Photochemical Conversion and Optoelectronic Materials, Technical Institute of Physics and Chemistry, Chinese Academy of Sciences, Beijing 100190, P. R. China;* orcid.org/0000-0002-5561-9922

Complete contact information is available at: https://pubs.acs.org/10.1021/jacsau.5c00115

Author Contributions

The manuscript was written through contributions of all authors. All authors have given approval to the final version of the paper. CRediT: **Shijie Li**: data curation, formal analysis, writing - original draft; **Hongrui Liu**: data curation, formal analysis, writing - original draft; **Guangbo Chen**: conceptualization, formal analysis, funding acquisition, supervision, writing- review and editing; **Li-Zhu Wu**: conceptualization, writing- review and editing; **Tierui Zhang**: conceptualization, funding acquisition, project administration, supervision, writing- review and editing.

Notes

The authors declare no competing financial interest.

ACKNOWLEDGMENTS

The authors are thankful for the financial support from the National Key R&D Program of China (2023YFA1507201, 2024YFA1510700), the National Natural Science Foundation of China (22421005, 52120105002, 52432006, 22088102), the International Partnership Program of Chinese Academy of Sciences (174GJHZ2024054MI), and the Liaoning Binhai Laboratory (LBLD-2024-06).

REFERENCES

(1) Vilanova, A.; Dias, P.; Lopes, T.; Mendes, A. The Route for Commercial Photoelectrochemical Water Splitting: a Review of Large-area Devices and Key Upscaling Challenges. *Chem. Soc. Rev.* **2024**, *53* (5), 2388−2434.

(2) Liu, Y.; Wang, Y.; Fornasiero, P.; Tian, G.; Strasser, P.; Yang, X.-Y. Long-term Durability of Seawater Electrolysis for Hydrogen: From Catalysts to Systems. *Angew. Chem., Int. Ed.* **2024**, *63* (47), No. e202412087.

(3) Mancuso, F.; Fornasiero, P.; Prato, M.; Melchionna, M.; Franco, F.; Filippini, G. Nanostructured Electrocatalysts for Organic Synthetic Transformations. *Nanoscale* **2024**, *16* (12), 5926−5940.
(4) Sportelli, G.; Marchi, M.; Fornasiero, P.; Filippini, G.; Franco, F.; Melchionna, M. Photoelectrocatalysis for Hydrogen Evolution Ventures into the World of Organic Synthesis. *Glob. Chall.* **2024**, *8* (6), 2400012.
(5) Yang, W.; Prabhakar, R. R.; Tan, J.; Tilley, S. D.; Moon, J. Strategies for Enhancing the Photocurrent, Photovoltage, and Stability of Photoelectrodes for Photoelectrochemical Water Splitting. *Chem. Soc. Rev.* **2019**, *48* (19), 4979−5015.
(6) Tang, R.; Zhou, S.; Zhang, Z.; Zheng, R.; Huang, J. Engineering Nanostructure-Interface of Photoanode Materials Toward Photoelectrochemical Water Oxidation. *Adv. Mater.* **2021**, *33* (17), 2005389.
(7) Li, Z.; Luo, W.; Zhang, M.; Feng, J.; Zou, Z. Photoelectrochemical Cells for Solar Hydrogen Production: Current State of Promising Photoelectrodes, Methods to Improve Their Properties, and Outlook. *Energy Environ. Sci.* **2013**, *6* (2), 347−370.
(8) Malapit, C. A.; Prater, M. B.; Cabrera-Pardo, J. R.; Li, M.; Pham, T. D.; McFadden, T. P.; Blank, S.; Minteer, S. D. Advances on the Merger of Electrochemistry and Transition Metal Catalysis for Organic Synthesis. *Chem. Rev.* **2022**, *122* (3), 3180−3218.
(9) Liu, B.; Wang, S.; Zhang, G.; Gong, Z.; Wu, B.; Wang, T.; Gong, J. Tandem Cells for Unbiased Photoelectrochemical Water Splitting. *Chem. Soc. Rev.* **2023**, *52* (14), 4644−4671.
(10) Miller, E. L. Photoelectrochemical Water Splitting. *Energy Environ. Sci.* **2015**, *8* (10), 2809−2810.
(11) Liu, S.; Wu, L.; Tang, D.; Xue, J.; Dang, K.; He, H.; Bai, S.; Ji, H.; Chen, C.; Zhang, Y.; et al. Transition from Sequential to Concerted Proton-Coupled Electron Transfer of Water Oxidation on Semiconductor Photoanodes. *J. Am. Chem. Soc.* **2023**, *145* (43), 23849−23858.
(12) Pornrungroj, C.; Andrei, V.; Reisner, E. Thermoelectric-Photoelectrochemical Water Splitting under Concentrated Solar Irradiation. *J. Am. Chem. Soc.* **2023**, *145* (25), 13709−13714.
(13) Wu, S. M.; Wu, L.; Denisov, N.; Badura, Z.; Zoppellaro, G.; Yang, X.-Y.; Schmuki, P. Pt Single Atoms on TiO_2 Can Catalyze Water Oxidation in Photoelectrochemical Experiments. *J. Am. Chem. Soc.* **2024**, *146* (24), 16363−16368.
(14) Yang, J.; Deng, C.; Lei, Y.; Duan, M.; Yang, Y.; Chen, X.; Yang, S.; Li, J.; Sheng, H.; Shi, W. Fe-N Co-Doped $BiVO_4$ Photoanode with Record Photocurrent for Water Oxidation. *Angew. Chem., Int. Ed.* **2025**, *64*, No. e202416340.
(15) Pan, L.; Dai, L.; Burton, O. J.; Chen, L.; Andrei, V.; Zhang, Y.; Ren, D.; Cheng, J.; Wu, L.; Frohna, K.; et al. High Carrier Mobility along the [111] Orientation in Cu_2O Photoelectrodes. *Nature* **2024**, *628* (8009), 765−770.
(16) King, A. J.; Bui, J. C.; Bell, A. T.; Weber, A. Z. Establishing the Role of Operating Potential and Mass Transfer in Multicarbon Product Generation for Photoelectrochemical CO_2 Reduction Cells Using a Cu Catalyst. *ACS Energy Lett.* **2022**, *7* (8), 2694−2700.
(17) Yeung, C. W. S.; Andrei, V.; Lee, T. H.; Durrant, J. R.; Reisner, E. Organic Semiconductor-$BiVO_4$ Tandem Devices for Solar-Driven H_2O and CO_2 Splitting. *Adv. Mater.* **2024**, *36* (35), 2404110.
(18) Zhang, Y.; Pan, D.; Tao, Y.; Shang, H.; Zhang, D.; Li, G.; Li, H. Photoelectrocatalytic Reduction of CO_2 to Syngas via SnO_x-enhanced Cu_2O Nanowires Photocathodes. *Adv. Funct. Mater.* **2022**, *32* (8), 2109600.
(19) Li, M.; Lu, Q.; Liu, M.; Yin, P.; Wu, C.; Li, H.; Zhang, Y.; Yao, S. Photoinduced Charge Separation via the Double-Electron Transfer Mechanism in Nitrogen Vacancies g-C_3N_5/BiOBr for the Photoelectrochemical Nitrogen Reduction. *ACS Appl. Mater. Interfaces* **2020**, *12* (34), 38266−38274.
(20) Sun, C.; Shao, Z.; Hu, Y.; Peng, Y.; Xie, Q. Photoelectrocatalysis Synthesis of Ammonia Based on a Ni-Doped MoS_2/Si Nanowires Photocathode and Porous Water with High N_2 Solubility. *ACS Appl. Mater. Interfaces* **2023**, *15* (19), 23085−23092.
(21) Bai, Y.; Lu, J.; Bai, H.; Fang, Z.; Wang, F.; Liu, Y.; Sun, D.; Luo, B.; Fan, W.; Shi, W. Understanding the Key Role of Vanadium in p-type $BiVO_4$ for Photoelectrochemical N_2 Fixation. *Chem. Eng. J.* **2021**, *414*, 128773.
(22) Peramaiah, K.; Ramalingam, V.; Fu, H. C.; Alsabban, M. M.; Ahmad, R.; Cavallo, L.; Tung, V.; Huang, K. W.; He, J. H. Optically and Electrocatalytically Decoupled Si Photocathodes with a Porous Carbon Nitride Catalyst for Nitrogen Reduction with Over 61.8% Faradaic Efficiency. *Adv. Mater.* **2021**, *33* (18), 2100812.
(23) Liu, D.; Kuang, Y. Particle-Based Photoelectrodes for PEC Water Splitting: Concepts and Perspectives. *Adv. Mater.* **2024**, *36* (37), 2311692.
(24) Cheng, W.-H.; de la Calle, A.; Atwater, H. A.; Stechel, E. B.; Xiang, C. Hydrogen from Sunlight and Water: A Side-by-Side Comparison between Photoelectrochemical and Solar Thermochemical Water-Splitting. *ACS Energy Lett.* **2021**, *6* (9), 3096−3113.
(25) Han, G. H.; Bang, J.; Park, G.; Choe, S.; Jang, Y. J.; Jang, H. W.; Kim, S. Y.; Ahn, S. H. Recent Advances in Electrochemical, Photochemical, and Photoelectrochemical Reduction of CO_2 to C_{2+} Products. *Small* **2023**, *19* (16), 2205765.
(26) Jang, G. Y.; Choi, Y. M.; Roh, S. H.; Wan, S.; Zhang, K.; Kwon, S. J.; Kim, J. K.; Park, J. H. Plasmon-Driven Reaction Selectivity Tuning for Photoelectrochemical H_2O_2 Production. *ACS Energy Lett.* **2023**, *8* (12), 5192−5200.
(27) Lu, Y.; Liu, T.-K.; Lin, C.; Kim, K. H.; Kim, E.; Yang, Y.; Fan, X.; Zhang, K.; Park, J. H. Nanoconfinement Enables Photoelectrochemical Selective Oxidation of Glycerol via the Microscale Fluid Effect. *Nano Lett.* **2024**, *24* (15), 4633−4640.
(28) Liu, T. K.; Jang, G. Y.; Kim, S.; Zhang, K.; Zheng, X. L.; Park, J. H. Organic Upgrading through Photoelectrochemical Reactions: Toward Higher Profits. *Small Methods* **2024**, *8* (2), 2300315.
(29) Huang, S.; Feng, F.; Huang, R. T.; Ouyang, T.; Liu, J. L.; Liu, Z. Q. Activating C-H Bonds by Tuning Fe Sites and an Interfacial Effect for Enhanced Methanol Oxidation. *Adv. Mater.* **2022**, *34* (50), 2208438.
(30) Huang, S.; Ouyang, T.; Zheng, B. F.; Dan, M.; Liu, Z. Q. Enhanced Photoelectrocatalytic Activities for CH_3OH-to-HCHO Conversion on Fe_2O_3/MoO_3: Fe-O-Mo Covalency Dominates the Intrinsic Activity. *Angew. Chem., Int. Ed.* **2021**, *60* (17), 9546−9552.
(31) Lin, C.; Shan, Z.; Dong, C.; Lu, Y.; Meng, W.; Zhang, G.; Cai, B.; Su, G.; Park, J. H.; Zhang, K. Covalent Organic Frameworks Bearing Ni Active Sites for Free Radical-mediated Photoelectrochemical Organic Transformations. *Sci. Adv.* **2023**, *9* (45), 9442.
(32) Lu, Y.; Lee, B. G.; Lin, C.; Liu, T.-K.; Wang, Z.; Miao, J.; Oh, S. H.; Kim, K. C.; Zhang, K.; Park, J. H. Solar-driven Highly Selective Conversion of Glycerol to Dihydroxyacetone Using Surface Atom Engineered $BiVO_4$ Photoanodes. *Nat. Commun.* **2024**, *15* (1), 5475.
(33) Xiao, Y.; Wang, M.; Liu, D.; Gao, J.; Ding, J.; Wang, H.; Yang, H. B.; Li, F.; Chen, M.; Xu, Y. Selective Photoelectrochemical Oxidation of Glycerol to Glyceric Acid on (002) Facets Exposed WO_3 Nanosheets. *Angew. Chem., Int. Ed.* **2024**, *136* (11), No. e202319685.
(34) Tian, Z.; Da, Y.; Wang, M.; Dou, X.; Cui, X.; Chen, J.; Jiang, R.; Xi, S.; Cui, B.; Luo, Y.; et al. Selective Photoelectrochemical Oxidation of Glucose to Glucaric Acid by Single Atom Pt Decorated Defective TiO_2. *Nat. Commun.* **2023**, *14* (1), 142.
(35) Ma, J.; Mao, K.; Low, J.; Wang, Z.; Xi, D.; Zhang, W.; Ju, H.; Qi, Z.; Long, R.; Wu, X.; et al. Efficient Photoelectrochemical Conversion of Methane into Ethylene Glycol by WO_3 Nanobar Arrays. *Angew. Chem., Int. Ed.* **2021**, *60* (17), 9357−9361.
(36) Woo, H. K.; Gautam, A. K.; Barroso-Martínez, J. S.; Baddorf, A. P.; Zhou, K.; Choi, Y. Y.; He, J. J.; Mironenko, A. V.; Rodríguez-López, J.; Cai, L. L. Defect Engineering of WO_3 by Rapid Flame Reduction for Efficient Photoelectrochemical Conversion of Methane into Liquid Oxygenates. *Nano Lett.* **2023**, *23* (24), 11493−11500.
(37) Nie, S.; Wu, L.; Zhang, Q.; Huang, Y.; Liu, Q.; Wang, X. High-entropy-perovskite Subnanowires for Photoelectrocatalytic Coupling of Methane to Acetic Acid. *Nat. Commun.* **2024**, *15* (1), 6669.

https://doi.org/10.1021/jacsau.5c00115
JACS Au 2025, 5, 2061−2075

(38) Amano, F.; Shintani, A.; Tsurui, K.; Mukohara, H.; Ohno, T.; Takenaka, S. Photoelectrochemical Homocoupling of Methane under Blue Light Irradiation. *ACS Energy Lett.* **2019**, *4* (2), 502−507.
(39) Wang, J.; Yang, C.; Gao, H.; Zuo, L.; Guo, Z.; Yang, P.; Li, S.; Tang, Z. Customized Photoelectrochemical C-N and C-P Formation Enabled by Tailored Deposition on Photoanodes. *Angew. Chem., Int. Ed.* **2024**, *63* (41), No. e202408901.
(40) Chen, Y.; He, Y.; Gao, Y.; Xue, J.; Qu, W.; Xuan, J.; Mo, Y. Scalable Decarboxylative Trifluoromethylation by Ion-Shielding Heterogeneous Photoelectrocatalysis. *Science* **2024**, *384* (6696), 670−676.
(41) Zhao, Y.; Deng, C.; Tang, D.; Ding, L.; Zhang, Y.; Sheng, H.; Ji, H.; Song, W.; Ma, W.; Chen, C.; et al. α-Fe_2O_3 as a Versatile and Efficient Oxygen Atom Transfer Catalyst in Combination with H_2O as The Oxygen Source. *Nat. Catal.* **2021**, *4* (8), 684−691.
(42) Zhao, Y.; Duan, M.; Deng, C.; Yang, J.; Yang, S.; Zhang, Y.; Sheng, H.; Li, Y.; Chen, C.; Zhao, J. Br^-/BrO^--Mediated Highly Efficient Photoelectrochemical Epoxidation of Alkenes on α-Fe_2O_3. *Nat. Commun.* **2023**, *14* (1), 1943.
(43) Ko, M.; Kim, Y.; Woo, J.; Lee, B.; Mehrotra, R.; Sharma, P.; Kim, J.; Hwang, S. W.; Jeong, H. Y.; Lim, H.; et al. Direct Propylene Epoxidation with Oxygen Using A Photo-Electro-Heterogeneous Catalytic System. *Nat. Catal.* **2022**, *5* (1), 37−44.
(44) Zhu, Y.; Li, X.; Wen, Z.; Zhao, R.; Chen, Z.; Zhang, Z.; Gao, H.; Wang, S.; Li, F. Highly Efficient Photoelectrochemical Alkene Epoxidation on a Dye-Sensitized Photoanode. *J. Am. Chem. Soc.* **2024**, *146* (31), 21903−21912.
(45) Liu, X.; Chen, Z.; Xu, S.; Liu, G.; Zhu, Y.; Yu, X.; Sun, L.; Li, F. Bromide-Mediated Photoelectrochemical Epoxidation of Alkenes Using Water as an Oxygen Source with Conversion Efficiency and Selectivity up to 100%. *J. Am. Chem. Soc.* **2022**, *144* (43), 19770−19777.
(46) Yang, J.; Zhao, Y. K.; Duan, M. Y.; Deng, C. Y.; Zhang, Y. F.; Lei, Y.; Li, J. K.; Song, W. J.; Chen, C. C.; Zhao, J. C. HCO_3^--mediated Highly Efficient Photoelectrochemical Dioxygenation of Aryl Alkenes: Triple Roles of HCO_3^--Derived Radicals. *Energy Environ. Sci.* **2024**, *17* (1), 183−189.
(47) Zhang, L.; Liardet, L.; Luo, J. S.; Ren, D.; Grätzel, M.; Hu, X. L. Photoelectrocatalytic Arene C-H Amination. *Nat. Catal.* **2019**, *2* (4), 366−373.
(48) Wang, J. H.; Li, X. B.; Li, J.; Lei, T.; Wu, H. L.; Nan, X. L.; Tung, C. H.; Wu, L. Z. Photoelectrochemical cell for P-H/C-H Cross-Coupling with Hydrogen Evolution. *Chem. Commun.* **2019**, *55* (70), 10376−10379.
(49) Lai, X. L.; Chen, M.; Wang, Y. Q.; Song, J. S.; Xu, H. C. Photoelectrochemical Asymmetric Catalysis Enables Direct and Enantioselective Decarboxylative Cyanation. *J. Am. Chem. Soc.* **2022**, *144*, 20201.
(50) Cai, C. Y.; Lai, X. L.; Wang, Y.; Hu, H. H.; Song, J. S.; Yang, Y.; Wang, C.; Xu, H. C. Photoelectrochemical Asymmetric Catalysis Enables Site- and Enantioselective Cyanation of Benzylic C-H Bonds. *Nat. Catal.* **2022**, *5* (10), 943−951.
(51) Nie, S. Y.; Wu, L.; Wang, X. Electron-Delocalization-Stabilized Photoelectrocatalytic Coupling of Methane by NiO-Polyoxometalate Sub-1 nm Heterostructures. *J. Am. Chem. Soc.* **2023**, *145* (43), 23681−23690.
(52) Wang, J. H.; Zuo, L. L.; Guo, Z. Y.; Yang, C. Y.; Jiang, Y. H.; Huang, X. W.; Wu, L. Z.; Tang, Z. Y. Al_2O_3-coated $BiVO_4$ Photoanodes for Photoelectrocatalytic Regioselective C-H Activation of Aromatic Amines. *Angew. Chem., Int. Ed.* **2023**, *62* (52), No. e202315478.
(53) Zou, L.; Xiang, S.; Sun, R.; Lu, Q. Selective C(sp^3)-H Arylation/Alkylation of Alkanes Enabled by Paired Electrocatalysis. *Nat. Commun.* **2023**, *14* (1), 7992.
(54) Xiong, P.; Ivlev, S. I.; Meggers, E. Photoelectrochemical Asymmetric Dehydrogenative [2 + 2] Cycloaddition between C-C Single and Double Bonds via the Activation of Two C(sp^3)-H Bonds. *Nat. Catal.* **2023**, *6* (12), 1186−1193.
(55) Gong, M.; Kim, J. K.; Zhao, X.; Li, Y.; Zhang, J.; Huang, M.; Wu, Y. Visible-light-induced α-oxyamination of 1,3-Dicarbonyls with TEMPO via a Photo(electro)catalytic Process Applying a DSSC Anode or in a DSSC System. *Green Chem.* **2019**, *21* (13), 3615−3620.
(56) Sendeku, M. G.; Shifa, T. A.; Dajan, F. T.; Ibrahim, K. B.; Wu, B.; Yang, Y.; Moretti, E.; Vomiero, A.; Wang, F. Frontiers in Photoelectrochemical Catalysis: A Focus on Valuable Product Synthesis. *Adv. Mater.* **2024**, *36* (21), 2308101.
(57) Li, P.; Zhang, T.; Mushtaq, M. A.; Wu, S.; Xiang, X.; Yan, D. Research Progress in Organic Synthesis by Means of Photoelectrocatalysis. *Chem. Rec.* **2021**, *21* (4), 841−857.
(58) Hardwick, T.; Qurashi, A.; Shirinfar, B.; Ahmed, N. Interfacial Photoelectrochemical Catalysis: Solar-Induced Green Synthesis of Organic Molecules. *ChemSusChem* **2020**, *13* (8), 1967−1973.
(59) Jin, C. D.; Han, M. X.; Wu, Y. H.; Wang, S. R. Solar-driven Photoelectrochemical Conversion of Biomass: Recent Progress, Mechanistic Insights and Potential Scalability. *Energy Environ. Sci.* **2024**, *17* (20), 7459−7511.
(60) Kumagai, H.; Tamaki, Y.; Ishitani, O. Photocatalytic Systems for CO_2 Reduction: Metal-Complex Photocatalysts and Their Hybrids with Photofunctional Solid Materials. *Acc. Chem. Res.* **2022**, *55* (7), 978−990.
(61) Fang, S.; Rahaman, M.; Bharti, J.; Reisner, E.; Robert, M.; Ozin, G. A.; Hu, Y. H. Photocatalytic CO_2 Reduction. *Nat. Rev. Methods Primers* **2023**, *3* (1), 61.
(62) Saha, P.; Amanullah, S.; Dey, A. Selectivity in Electrochemical CO_2 Reduction. *Acc. Chem. Res.* **2022**, *55* (2), 134−144.
(63) Halmann, M. Photoelectrochemical Reduction of Aqueous Carbon Dioxide on P-type Gallium Phosphide in Liquid Junction Solar Cells. *Nature* **1978**, *275* (5676), 115−116.
(64) Shang, B.; Rooney, C. L.; Gallagher, D. J.; Wang, B. T.; Krayev, A.; Shema, H.; Leitner, O.; Harmon, N. J.; Xiao, L.; Sheehan, C.; et al. Aqueous Photoelectrochemical CO_2 Reduction to CO and Methanol over a Silicon Photocathode Functionalized with a Cobalt Phthalocyanine Molecular Catalyst. *Angew. Chem., Int. Ed.* **2023**, *62* (4), No. e202215213.
(65) Liu, B.; Wang, T.; Wang, S.; Zhang, G.; Zhong, D.; Yuan, T.; Dong, H.; Wu, B.; Gong, J. Back-illuminated Photoelectrochemical Flow Cell for Efficient CO_2 Reduction. *Nat. Commun.* **2022**, *13* (1), 7111.
(66) Pati, P. B.; Wang, R.; Boutin, E.; Diring, S.; Jobic, S.; Barreau, N.; Odobel, F.; Robert, M. Photocathode Functionalized with a Molecular Cobalt Catalyst for Selective Carbon Dioxide Reduction in Water. *Nat. Commun.* **2020**, *11* (1), 3499.
(67) Andrei, V.; Jagt, R. A.; Rahaman, M.; Lari, L.; Lazarov, V. K.; MacManus-Driscoll, J. L.; Hoye, R. L. Z.; Reisner, E. Long-term Solar Water and CO_2 Splitting with Photoelectrochemical BiOI-$BiVO_4$ Tandems. *Nat. Mater.* **2022**, *21* (8), 864−868.
(68) Andrei, V.; Reuillard, B.; Reisner, E. Bias-free Solar Syngas Production by Integrating a Molecular Cobalt Catalyst with Perovskite-$BiVO_4$ Tandems. *Nat. Mater.* **2020**, *19* (2), 189−194.
(69) Khan, B.; Faheem, M. B.; Peramaiah, K.; Nie, J.; Huang, H.; Li, Z.; Liu, C.; Huang, K.-W.; He, J.-H. Unassisted Photoelectrochemical CO_2-to-liquid Fuel Splitting over 12% Solar Conversion Efficiency. *Nat. Commun.* **2024**, *15* (1), 6990.
(70) Xia, M.; Pan, L.; Liu, Y.; Gao, J.; Li, J.; Mensi, M.; Sivula, K.; Zakeeruddin, S. M.; Ren, D.; Grätzel, M. Efficient Cu_2O Photocathodes for Aqueous Photoelectrochemical CO_2 Reduction to Formate and Syngas. *J. Am. Chem. Soc.* **2023**, *145* (51), 27939−27949.
(71) Kato, N.; Mizuno, S.; Shiozawa, M.; Nojiri, N.; Kawai, Y.; Fukumoto, K.; Morikawa, T.; Takeda, Y. A Large-sized Cell for Solar-driven CO_2 Conversion with a Solar-to-Formate Conversion Efficiency of 7.2%. *Joule* **2021**, *5* (3), 687−705.
(72) Shang, B.; Zhao, F.; Suo, S.; Gao, Y.; Sheehan, C.; Jeon, S.; Li, J.; Rooney, C. L.; Leitner, O.; Xiao, L.; et al. Tailoring Interfaces for Enhanced Methanol Production from Photoelectrochemical CO_2 Reduction. *J. Am. Chem. Soc.* **2024**, *146* (3), 2267−2274.

https://doi.org/10.1021/jacsau.5c00115
JACS Au 2025, 5, 2061−2075

(73) Pan, Z.; Han, E.; Zheng, J.; Lu, J.; Wang, X.; Yin, Y.; Waterhouse, G. I. N.; Wang, X.; Li, P. Highly Efficient Photoelectrocatalytic Reduction of CO_2 to Methanol by a p-n Heterojunction CeO_2/CuO/Cu Catalyst. *Nano Micro Lett.* **2020**, *12* (1), 18.
(74) Liu, H.; Zhou, X.; Xu, K.; Zhang, H.; Wang, H.; Zhou, H.; Chen, H. Mesoporous TS-1 Zeolite-confined Metal Oxides Photocathode for Efficient Reduction of Carbon Dioxide to Methanol. *Chem. Eng. J.* **2024**, *489*, 151483.
(75) Zhou, B.; Ou, P.; Pant, N.; Cheng, S.; Vanka, S.; Chu, S.; Rashid, R. T.; Botton, G.; Song, J.; Mi, Z. Highly Efficient Binary Copper-iron Catalyst for Photoelectrochemical Carbon Dioxide Reduction toward Methane. *Proc. Natl. Acad. Sci. U.S.A.* **2020**, *117* (3), 1330−1338.
(76) Kim, C.; King, A. J.; Aloni, S.; Toma, F. M.; Weber, A. Z.; Bell, A. T. Codesign of an Integrated Metal-Insulator-Semiconductor Photocathode for Photoelectrochemical Reduction of CO_2 to Ethylene. *Energy Environ. Sci.* **2023**, *16* (7), 2968−2976.
(77) Liu, G.; Zheng, F.; Li, J.; Zeng, G.; Ye, Y.; Larson, D. M.; Yano, J.; Crumlin, E. J.; Ager, J. W.; Wang, L.-w.; et al. Investigation and Mitigation of Degradation Mechanisms in Cu_2O Photoelectrodes for CO_2 Reduction to Ethylene. *Nat. Energy* **2021**, *6* (12), 1124−1132.
(78) Wan, W.; Zhang, Q.; Wei, Y.; Cao, Y.; Hou, J.; Liu, C.; Hong, L.; Gao, H.; Chen, J.; Jing, H. P-n Heterojunctions of Si@WO_3 Mimicking Thylakoid for Photoelectrocatalytic CO_2 Reduction to C_{2+} Products-Morphology Control. *Chem. Eng. J.* **2023**, *454*, 140122.
(79) Rahaman, M.; Andrei, V.; Wright, D.; Lam, E.; Pornrungroj, C.; Bhattacharjee, S.; Pichler, C. M.; Greer, H. F.; Baumberg, J. J.; Reisner, E. Solar-driven Liquid Multi-Carbon Fuel Production Using a Standalone Perovskite-$BiVO_4$ Artificial Leaf. *Nat. Energy* **2023**, *8* (6), 629−638.
(80) Wang, X.; Gao, C.; Low, J.; Mao, K.; Duan, D.; Chen, S.; Ye, R.; Qiu, Y.; Ma, J.; Zheng, X. Efficient Photoelectrochemical CO_2 Conversion for Selective Acetic Acid Production. *Sci. Bull.* **2021**, *66* (13), 1296−1304.
(81) Ta, X. M. C.; Daiyan, R.; Nguyen, T. K. A.; Amal, R.; Tran-Phu, T.; Tricoli, A. Alternatives to Water Photooxidation for Photoelectrochemical Solar Energy Conversion and Green H_2 Production. *Adv. Energy Mater.* **2022**, *12* (42), 2201358.
(82) Yu, J.; González-Cobos, J.; Dappozze, F.; Grimaldos-Osorio, N.; Vernoux, P.; Caravaca, A.; Guillard, C. First PEM Photoelectrolyser for the Simultaneous Selective Glycerol Valorization into Value-added Chemicals and Hydrogen Generation. *Appl. Catal., B* **2023**, *327*, 122465.
(83) Bharath, G.; Rambabu, K.; Hai, A.; Ponpandian, N.; Schmidt, J. E.; Dionysiou, D. D.; Abu Haija, M.; Banat, F. Dual-functional Paired Photoelectrocatalytic System for the Photocathodic Reduction of CO_2 to Fuels and the Anodic Oxidation of Furfural to Value-added Chemicals. *Appl. Catal., B* **2021**, *298*, 120520.
(84) Antón-García, D.; Edwardes Moore, E.; Bajada, M. A.; Eisenschmidt, A.; Oliveira, A. R.; Pereira, I. A. C.; Warnan, J.; Reisner, E. Photoelectrochemical Hybrid Cell for Unbiased CO_2 Reduction Coupled to Alcohol Oxidation. *Nat. Synth.* **2022**, *1* (1), 77−86.
(85) Pan, Y.; Zhang, H.; Zhang, B.; Gong, F.; Feng, J.; Huang, H.; Vanka, S.; Fan, R.; Cao, Q.; Shen, M.; et al. Renewable Formate from Sunlight, Biomass and Carbon Dioxide in a Photoelectrochemical Cell. *Nat. Commun.* **2023**, *14* (1), 1013.
(86) Luo, L.; Chen, W.; Xu, S.-M.; Yang, J.; Li, M.; Zhou, H.; Xu, M.; Shao, M.; Kong, X.; Li, Z. Selective Photoelectrocatalytic Glycerol Oxidation to Dihydroxyacetone via Enhanced Middle Hydroxyl Adsorption over a Bi_2O_3-Incorporated Catalyst. *J. Am. Chem. Soc.* **2022**, *144* (17), 7720−7730.
(87) Liu, Y.; Wang, M.; Zhang, B.; Yan, D.; Xiang, X. Mediating the Oxidizing Capability of Surface-Bound Hydroxyl Radicals Produced by Photoelectrochemical Water Oxidation to Convert Glycerol into Dihydroxyacetone. *ACS Catal.* **2022**, *12* (12), 6946−6957.
(88) Lin, J.-A.; Roh, I.; Yang, P. Photochemical Diodes for Simultaneous Bias-Free Glycerol Valorization and Hydrogen Evolution. *J. Am. Chem. Soc.* **2023**, *145* (24), 12987−12991.
(89) Wang, L.; Chen, Z.; Zhao, Q.; Wen, N.; Liang, S.; Jiao, X.; Xia, Y.; Chen, D. Modulating Surface Oxygen Valence States via Interfacial Potential in $BiVO_4$/CoO_x/Au Photoanode for Enhanced Selective Photoelectrochemical Oxidation of Glycerol to Dihydroxyacetone. *Adv. Funct. Mater.* **2024**, *34* (49), 2409349.
(90) Liu, Y.; Shang, H.; Zhang, B.; Yan, D.; Xiang, X. Surface Fluorination of $BiVO_4$ for the Photoelectrochemical Oxidation of Glycerol to Formic Acid. *Nat. Commun.* **2024**, *15* (1), 8155.
(91) Lin, C.; Dong, C.; Kim, S.; Lu, Y.; Wang, Y.; Yu, Z.; Gu, Y.; Gu, Z.; Lee, D. K.; Zhang, K.; et al. Photo-Electrochemical Glycerol Conversion over a Mie Scattering Effect Enhanced Porous $BiVO_4$ Photoanode. *Adv. Mater.* **2023**, *35* (15), 2209955.
(92) Kim, J.; Lin, J.-A.; Kim, J.; Roh, I.; Lee, S.; Yang, P. A Red-light-Powered Silicon Nanowire Biophotochemical Diode for Simultaneous CO_2 Reduction and Glycerol Valorization. *Nat. Catal.* **2024**, *7* (9), 977−986.
(93) Andrei, V.; Roh, I.; Lin, J.-A.; Lee, J.; Shan, Y.; Lin, C.-K.; Shelton, S.; Reisner, E.; Yang, P. Perovskite-driven Solar C_2 Hydrocarbon Synthesis from CO_2. *Nat. Catal.* **2025**, *8* (2), 137−146.
(94) Balog, A.; Kecsenovity, E.; Samu, G. F.; He, J.; Fekete, D.; Janaky, C. Paired Photoelectrochemical Conversion of CO_2/H_2O and Glycerol at High Rate. *Nat. Catal.* **2024**, *7* (5), 522−535.
(95) Andrady, A. L.; Barnes, P. W.; Bornman, J. F.; Gouin, T.; Madronich, S.; White, C. C.; Zepp, R. G.; Jansen, M. A. K. Oxidation and Fragmentation of Plastics in a Changing Environment; from UV-radiation to Biological Degradation. *Sci. Total Environ.* **2022**, *851*, 158022.
(96) Chu, S.; Zhang, B.; Zhao, X.; Soo, H. S.; Wang, F.; Xiao, R.; Zhang, H. Photocatalytic Conversion of Plastic Waste: From Photodegradation to Photosynthesis. *Adv. Energy Mater.* **2022**, *12* (22), 2200435.
(97) Cao, R.; Zhang, M.-Q.; Hu, C.; Xiao, D.; Wang, M.; Ma, D. Catalytic Oxidation of Polystyrene to Aromatic Oxygenates over a Graphitic Carbon Nitride Catalyst. *Nat. Commun.* **2022**, *13* (1), 4809.
(98) Ragaert, K.; Delva, L.; Van Geem, K. Mechanical and Chemical Recycling of Solid Plastic Waste. *Waste Manage.* **2017**, *69*, 24−58.
(99) Wang, X.; Wang, W.; Wang, S.; Yang, Y.; Li, H.; Sun, J.; Gu, X.; Zhang, S. Self-intumescent Polyelectrolyte for Flame Retardant Poly (Lactic Acid) Nonwovens. *J. Cleaner Prod.* **2021**, *282*, 124497.
(100) Anh Nguyen, T. K.; Trân-Phú, T.; Daiyan, R.; Minh Chau Ta, X.; Amal, R.; Tricoli, A. From Plastic Waste to Green Hydrogen and Valuable Chemicals Using Sunlight and Water. *Angew. Chem., Int. Ed.* **2024**, *63* (32), No. e202401746.
(101) Li, T.; Vijeta, A.; Casadevall, C.; Gentleman, A. S.; Euser, T.; Reisner, E. Bridging Plastic Recycling and Organic Catalysis: Photocatalytic Deconstruction of Polystyrene via a C-H Oxidation Pathway. *ACS Catal.* **2022**, *12* (14), 8155−8163.
(102) Zhang, S.; Li, H.; Wang, L.; Liu, J.; Liang, G.; Davey, K.; Ran, J.; Qiao, S.-Z. Boosted Photoreforming of Plastic Waste via Defect-Rich $NiPS_3$ Nanosheets. *J. Am. Chem. Soc.* **2023**, *145* (11), 6410−6419.
(103) Du, M.; Zhang, Y.; Kang, S.; Guo, X.; Ma, Y.; Xing, M.; Zhu, Y.; Chai, Y.; Qiu, B. Trash to Treasure: Photoreforming of Plastic Waste into Commodity Chemicals and Hydrogen over MoS_2-Tipped CdS Nanorods. *ACS Catal.* **2022**, *12* (20), 12823−12832.
(104) Zhang, B.; Zhang, H.; Pan, Y.; Shao, J.; Wang, X.; Jiang, Y.; Xu, X.; Chu, S. Photoelectrochemical Conversion of Plastic Waste into High-value Chemicals Coupling Hydrogen Production. *Chem. Eng. J.* **2023**, *462*, 142247.
(105) Li, X.; Wang, J.; Sun, M.; Qian, X.; Zhao, Y. Ti-Fe_2O_3/$Ni(OH)_x$ as an Efficient and Durable Photoanode for the Photoelectrochemical Catalysis of PET Plastic to Formic Acid. *J. Energy Chem.* **2023**, *78*, 487−496.
(106) Bhattacharjee, S.; Andrei, V.; Pornrungroj, C.; Rahaman, M.; Pichler, C. M.; Reisner, E. Reforming of Soluble Biomass and Plastic

https://doi.org/10.1021/jacsau.5c00115
JACS Au 2025, 5, 2061−2075

Derived Waste Using a Bias-Free $Cu_{30}Pd_{70}$|Perovskite|Pt Photoelectrochemical Device. *Adv. Funct. Mater.* **2022**, *32* (7), 2109313.
(107) Li, X.; Wang, J.; Zhang, T.; Wang, T.; Zhao, Y. Photoelectrochemical Catalysis of Waste Polyethylene Terephthalate Plastic to Coproduce Formic Acid and Hydrogen. *ACS Sustain. Chem. Eng.* **2022**, *10* (29), 9546−9552.
(108) Feng, X.; Yang, L.; Zhang, L. Sustainable Solar- and Electro-driven Rroduction of High Concentration H_2O_2 Coupled to Electrocatalytic Upcycling of Polyethylene Terephthalate Plastic Waste. *Chem. Eng. J.* **2024**, *482*, 149191.
(109) Lin, C.-Y.; Huang, S.-C.; Lin, Y.-G.; Hsu, L.-C.; Yi, C.-T. Electrosynthesized Ni-P Nanospheres with High Activity and Selectivity Towards Photoelectrochemical Plastics Reforming. *Appl. Catal., B* **2021**, *296*, 120351.
(110) Quilumbaquin, W.; Castillo-Cabrera, G. X.; Borrero-González, L. J.; Mora, J. R.; Valle, V.; Debut, A.; Loor-Urgilés, L. D.; Espinoza-Montero, P. J. Photoelectrocatalytic Degradation of High-density Polyethylene Microplastics on TiO_2-modified Boron-Doped Diamond Photoanode. *iScience* **2024**, *27* (3), 109192.
(111) Zhao, H.; Zhao, X.; Zhang, J.; Anandita, S.; Liu, W.; Koh, S. W.; Yu, S.; Li, C.; Chen, Z.; Xu, R.; et al. Solar-Driven Photoelectrochemical Upcycling of Polyimide Plastic Waste with Safe Green Hydrogen Generation. *Adv. Energy Mater.* **2024**, *14* (41), 2400037.
(112) Bhattacharjee, S.; Rahaman, M.; Andrei, V.; Miller, M.; Rodríguez-Jiménez, S.; Lam, E.; Pornrungroj, C.; Reisner, E. Photoelectrochemical CO_2-to-Fuel Conversion with Simultaneous Plastic Reforming. *Nat. Synth.* **2023**, *2* (2), 182−192.
(113) Ren, Y.; Li, S.; Yu, C.; Zheng, Y.; Wang, C.; Qian, B.; Wang, L.; Fang, W.; Sun, Y.; Qiu, J. NH_3 Electrosynthesis from N_2 Molecules: Progresses, Challenges, and Future Perspectives. *J. Am. Chem. Soc.* **2024**, *146* (10), 6409−6421.
(114) Mateo, D.; Sousa, A.; Zakharzhevskii, M.; Gascon, J. Challenges and Opportunities for the Photo-(thermal) Synthesis of Ammonia. *Green Chem.* **2024**, *26* (3), 1041−1061.
(115) Li, W.-Q.; Xu, M.; Chen, J.-S.; Ye, T.-N. Enabling Sustainable Ammonia Synthesis: From Nitrogen Activation Strategies to Emerging Materials. *Adv. Mater.* **2024**, *36* (40), 2408434.
(116) Ali, M.; Zhou, F.; Chen, K.; Kotzur, C.; Xiao, C.; Bourgeois, L.; Zhang, X.; MacFarlane, D. R. Nanostructured Photoelectrochemical Solar Cell for Nitrogen Reduction Using Plasmon-Enhanced Black Silicon. *Nat. Commun.* **2016**, *7* (1), 11335.
(117) Li, C.; Wang, T.; Zhao, Z.-J.; Yang, W.; Li, J.-F.; Li, A.; Yang, Z.; Ozin, G. A.; Gong, J. Back Cover: Promoted Fixation of Molecular Nitrogen with Surface Oxygen Vacancies on Plasmon-Enhanced TiO_2 Photoelectrodes. *Angew. Chem., Int. Ed.* **2018**, *57* (19), 5556−5556.
(118) Wang, B.; Yao, L.; Xu, G.; Zhang, X.; Wang, D.; Shu, X.; Lv, J.; Wu, Y.-C. Highly Efficient Photoelectrochemical Synthesis of Ammonia Using Plasmon-Enhanced Black Silicon under Ambient Conditions. *ACS Appl. Mater. Interfaces* **2020**, *12* (18), 20376−20382.
(119) Li, P.; Liu, Y.; Mushtaq, M. A.; Yan, D. Recent Progress in Ammonia Synthesis Based on Photoelectrocatalysis. *Inorg. Chem. Front.* **2023**, *10* (16), 4650−4667.
(120) Kim, C. H.; Kim, J.; Hollmann, F.; Park, C. B. Photoelectrocatalytic N_2 Fixation and C-H Oxyfunctionalization Driven by H_2O Oxidation. *Appl. Catal., B* **2023**, *336*, 122925.
(121) Zhang, H.; Wang, H.; Cao, X.; Chen, M.; Liu, Y.; Zhou, Y.; Huang, M.; Xia, L.; Wang, Y.; Li, T.; et al. Unveiling Cutting-Edge Developments in Electrocatalytic Nitrate-to-Ammonia Conversion. *Adv. Mater.* **2024**, *36* (16), 2312746.
(122) Du, C.; Lu, S.; Wang, J.-a.; Wang, X.; Wang, M.; Fruehwald, H. M.; Wang, L.; Zhang, B.; Guo, T.; Mills, J. P.; et al. Selectively Reducing Nitrate into NH_3 in Neutral Media by PdCu Single-Atom Alloy Electrocatalysis. *ACS Catal.* **2023**, *13* (16), 10560−10569.
(123) Huang, H.; Peramaiah, K.; Huang, K.-W. Rethinking Nitrate Reduction: Redirecting Electrochemical Efforts from Ammonia to Nitrogen for Realistic Environmental Impacts. *Energy Environ. Sci.* **2024**, *17* (8), 2682−2685.
(124) Kim, H. E.; Kim, J.; Ra, E. C.; Zhang, H.; Jang, Y. J.; Lee, J. S. Photoelectrochemical Nitrate Reduction to Ammonia on Ordered Silicon Nanowire Array Photocathodes. *Angew. Chem., Int. Ed.* **2022**, *61* (25), No. e202204117.
(125) Wang, F.; Ding, Q.; Ding, J.; Bai, Y.; Bai, H.; Fan, W. Frustrated Lewis Pairs Boosting Photoelectrochemical Nitrate Reduction over $ZnIn_2S_4/BiVO_4$ Heterostructure. *Chem. Eng. J.* **2022**, *450*, 138260.
(126) Zhou, S.; Sun, K.; Toe, C. Y.; Yin, J.; Huang, J.; Zeng, Y.; Zhang, D.; Chen, W.; Mohammed, O. F.; Hao, X.; et al. Engineering a Kesterite-Based Photocathode for Photoelectrochemical Ammonia Synthesis from NO_X Reduction. *Adv. Mater.* **2022**, *34* (29), 2201670.
(127) Bai, H.; Wang, F.; Ding, Q.; Xie, W.; Li, H.; Zheng, G.; Fan, W. Construction of Frustrated Lewis Pair Sites in CeO_2-C/$BiVO_4$ for Photoelectrochemical Nitrate Reduction. *Inorg. Chem.* **2023**, *62* (5), 2394−2403.
(128) Ren, S.; Gao, R.-T.; Nguyen, N. T.; Wang, L. Enhanced Charge Carrier Dynamics on Sb_2Se_3 Photocathodes for Efficient Photoelectrochemical Nitrate Reduction to Ammonia. *Angew. Chem., Int. Ed.* **2024**, *63* (11), No. e202317414.
(129) Ren, S.; Gao, R.-T.; Yu, J.; Yang, Y.; Liu, X.; Wu, L.; Wang, L. Enhanced Charge-Carrier Dynamics and Efficient Photoelectrochemical Nitrate-to-Ammonia Conversion on Antimony Sulfide-Based Photocathodes. *Angew. Chem., Int. Ed.* **2024**, *63* (48), No. e202409693.
(130) Li, Y.; Zhang, Q.; Dai, H.; He, D.; Ke, Z.; Xiao, X. Photoelectrochemical Nitrate Denitrification Towards Acidic Ammonia Synthesis on Copper-decorated Black Silicon. *Energy Environ. Sci.* **2024**, *17* (23), 9233−9243.
(131) Fang, Y.; Li, M.; Gao, Y.; Wen, Y.; Shan, B. Static Organic p-n Junctions in Photoelectrodes for Solar Ammonia Production with 86% Internal Quantum Efficiency. *Angew. Chem., Int. Ed.* **2025**, *64* (3), No. e202415729.
(132) Song, Y. R.; Wu, Y. Z.; Cao, S. Y.; Zhang, Y. X.; Luo, D. G.; Gao, J. F.; Li, Z. W.; Sun, L. C.; Hou, J. G. Simultaneous Photoelectrocatalytic Oxidation and Nitrite-Ammonia Conversion with Artificial Photoelectrochemistry Cells. *Adv. Energy Mater.* **2022**, *12* (48), 2201782.
(133) Tayyebi, A.; Mehrotra, R.; Mubarok, M. A.; Kim, J.; Zafari, M.; Tayebi, M.; Oh, D.; Lee, S.-h.; Matthews, J. E.; Lee, S.-W.; et al. Bias-free Solar NH_3 Production by Perovskite-Based Photocathode Coupled to Valorization of Glycerol. *Nat. Catal.* **2024**, *7* (5), 510−521.
(134) Dixit, R. J.; Singh, A.; Ramani, V. K.; Basu, S. Electrocatalytic Hydrogenation of Furfural Paired with Photoelectrochemical Oxidation of Water and Furfural in Batch and Flow Cells. *React. Chem. Eng.* **2021**, *6* (12), 2342−2353.
(135) Wang, D.; Lee, S. H.; Han, S.; Kim, J.; Trang, N. V. T.; Kim, K.; Choi, E. G.; Boonmongkolras, P.; Lee, Y. W.; Shin, B.; et al. Lignin-Fueled Photoelectrochemical Platform for Light-Driven Redox Biotransformation. *Green Chem.* **2020**, *22* (15), 5151−5160.
(136) Choi, D. S.; Kim, J.; Hollmann, F.; Park, C. B. Solar-Assisted eBiorefinery: Photoelectrochemical Pairing of Oxyfunctionalization and Hydrogenation Reactions. *Angew. Chem., Int. Ed.* **2020**, *59* (37), 15886−15890.
(137) Kim, J.; Um, Y.; Han, S.; Hilberath, T.; Kim, Y. H.; Hollmann, F.; Park, C. B. Unbiased Photoelectrode Interfaces for Solar Coupling of Lignin Oxidation with Biocatalytic C=C Bond Hydrogenation. *ACS Appl. Mater. Interfaces* **2022**, *14* (9), 11465−11473.
(138) Kim, J.; Jang, J.; Hilberath, T.; Hollmann, F.; Park, C. B. Photoelectrocatalytic Biosynthesis Fuelled by Microplastics. *Nat. Synth.* **2022**, *1* (10), 776−786.
(139) Hoque, M. A.; Gerken, J. B.; Stahl, S. S. Synthetic Dioxygenase Reactivity by Pairing Electrochemical Oxygen Reduction and Water Oxidation. *Science* **2024**, *383* (6679), 173−178.
(140) Sheng, H.; Janes, A. N.; Ross, R. D.; Hofstetter, H.; Lee, K.; Schmidt, J. R.; Jin, S. Linear Paired Electrochemical Valorization of Glycerol Enabled by the Electro-Fenton Process Using a Stable $NiSe_2$ Cathode. *Nat. Catal.* **2022**, *5* (8), 716−725.

https://doi.org/10.1021/jacsau.5c00115
JACS Au 2025, 5, 2061−2075